BROOKHAVEN NATIONAL LABORATORY

Hydrodynamics: state of the art

Chun Shen
Brookhaven National Lab

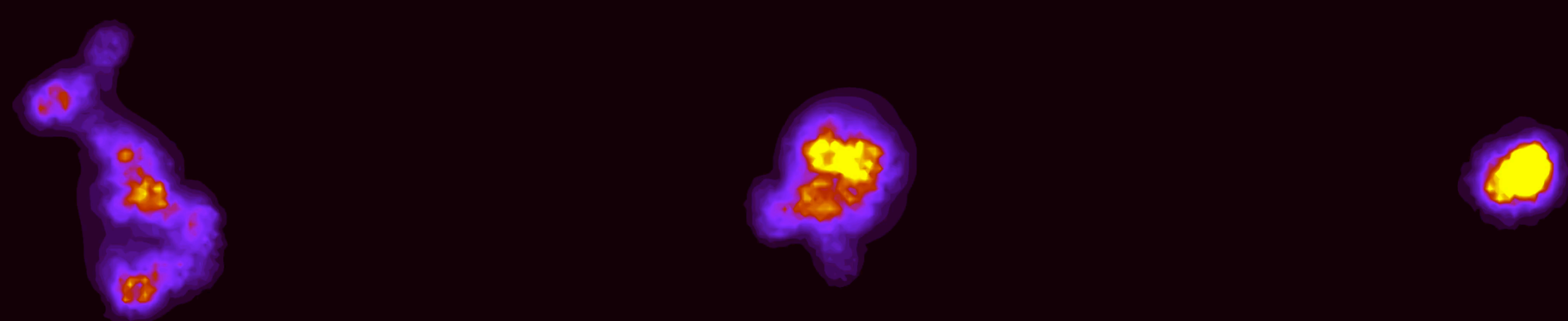

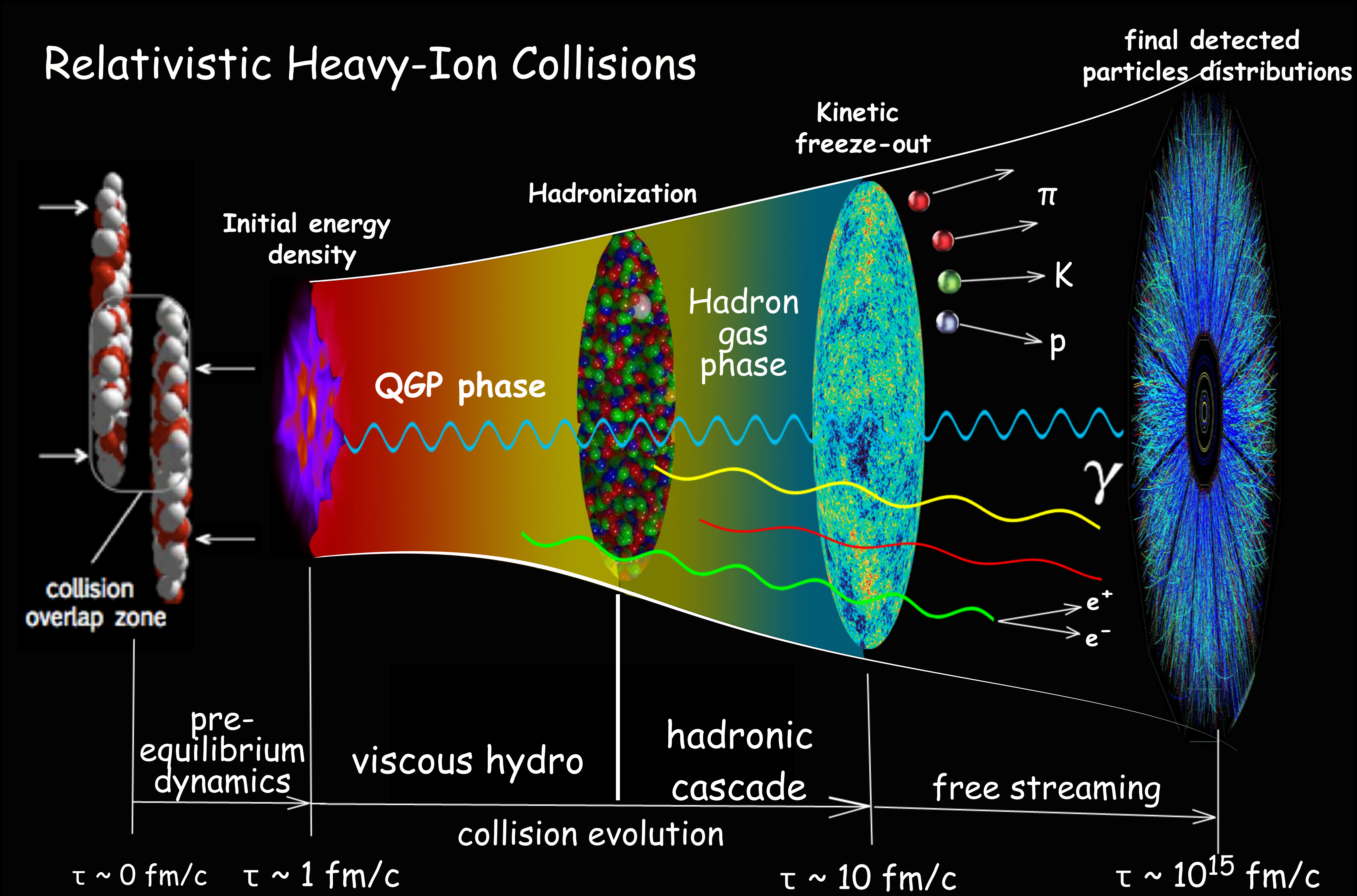
Relativistic Heavy-Ion Collisions
final detected particles distributions
Kinetic freeze-out
Hadronization
Initial energy density
π
K
p
Hadron gas phase
QGP phase
γ
collision overlap zone
e+
e−
pre-equilibrium dynamics
viscous hydro
hadronic cascade
free streaming
collision evolution
τ ~ 0 fm/c
τ ~ 1 fm/c
τ ~ 10 fm/c
τ ~ 10^15 fm/c

A blowing wind from hydrodynamics

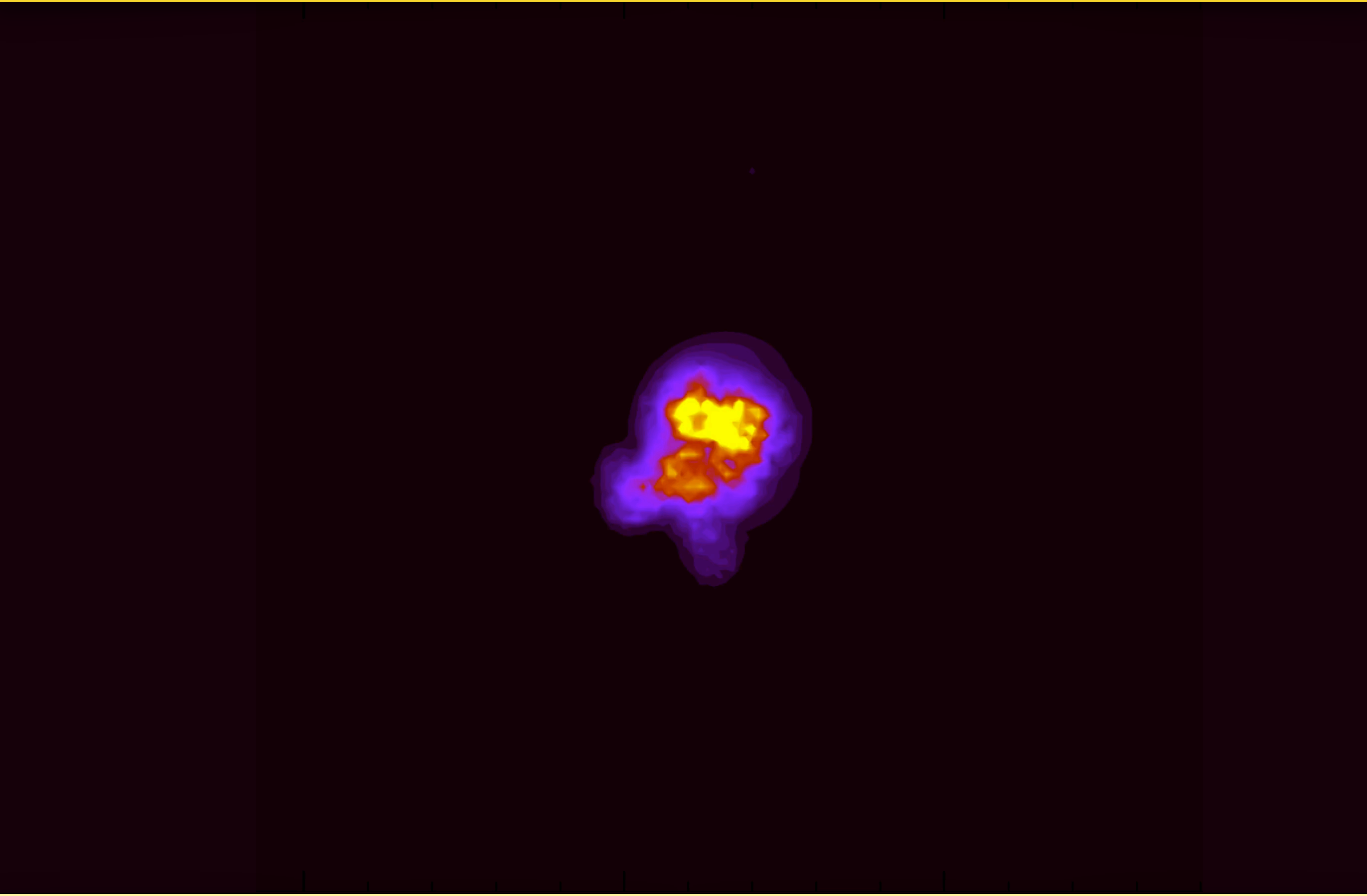

Identified particle spectra

S. McDonald, C. Shen, F. Fillion-Gourdeau, S. Jeon and C. Gale, Phys. Rev. C 95, 064913 (2017)

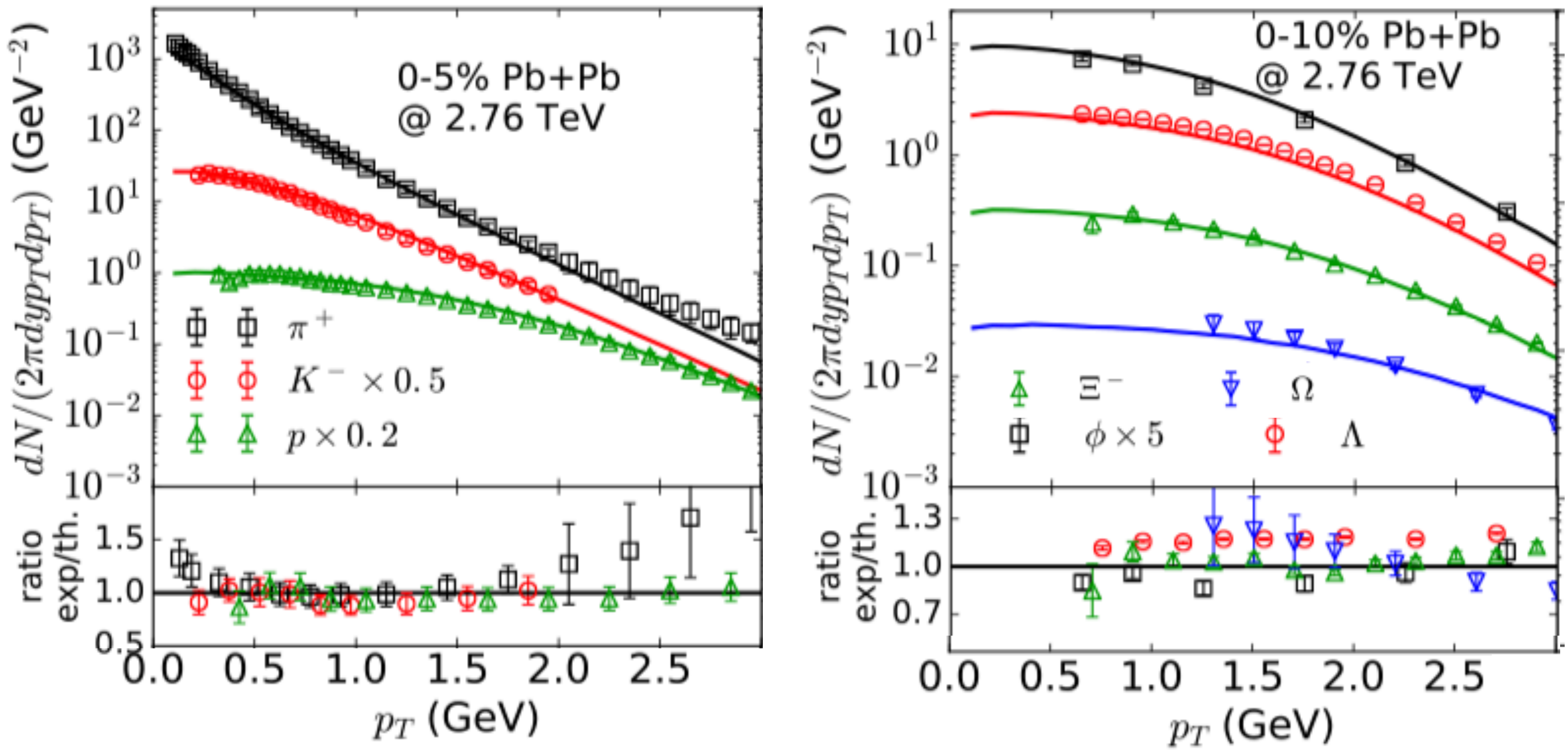

- Hydrodynamic simulations can describe a zoo of identified particle spectra within 30% accuracy

Anisotropic flow

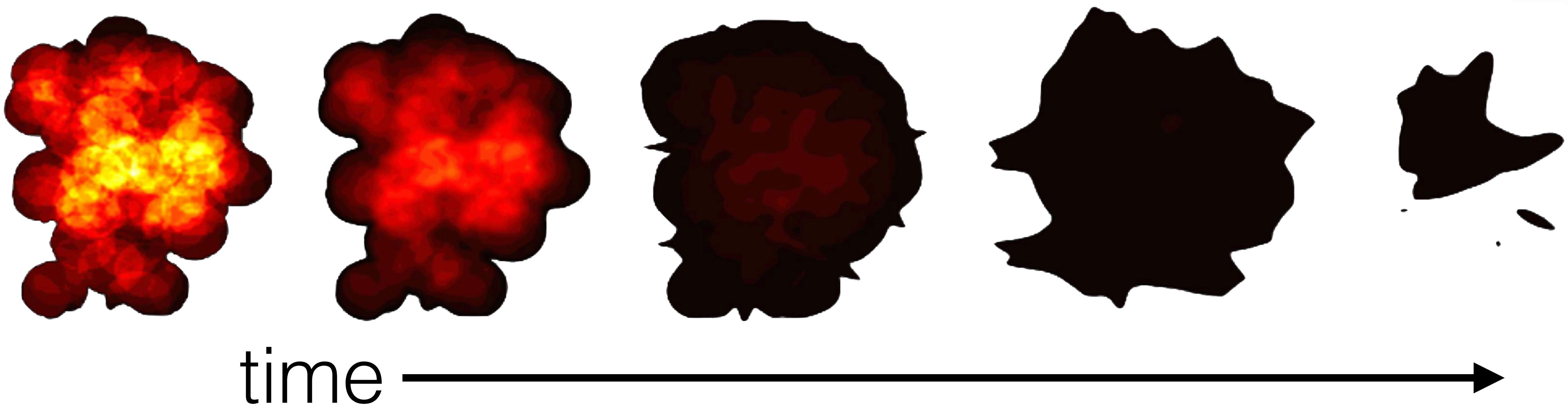

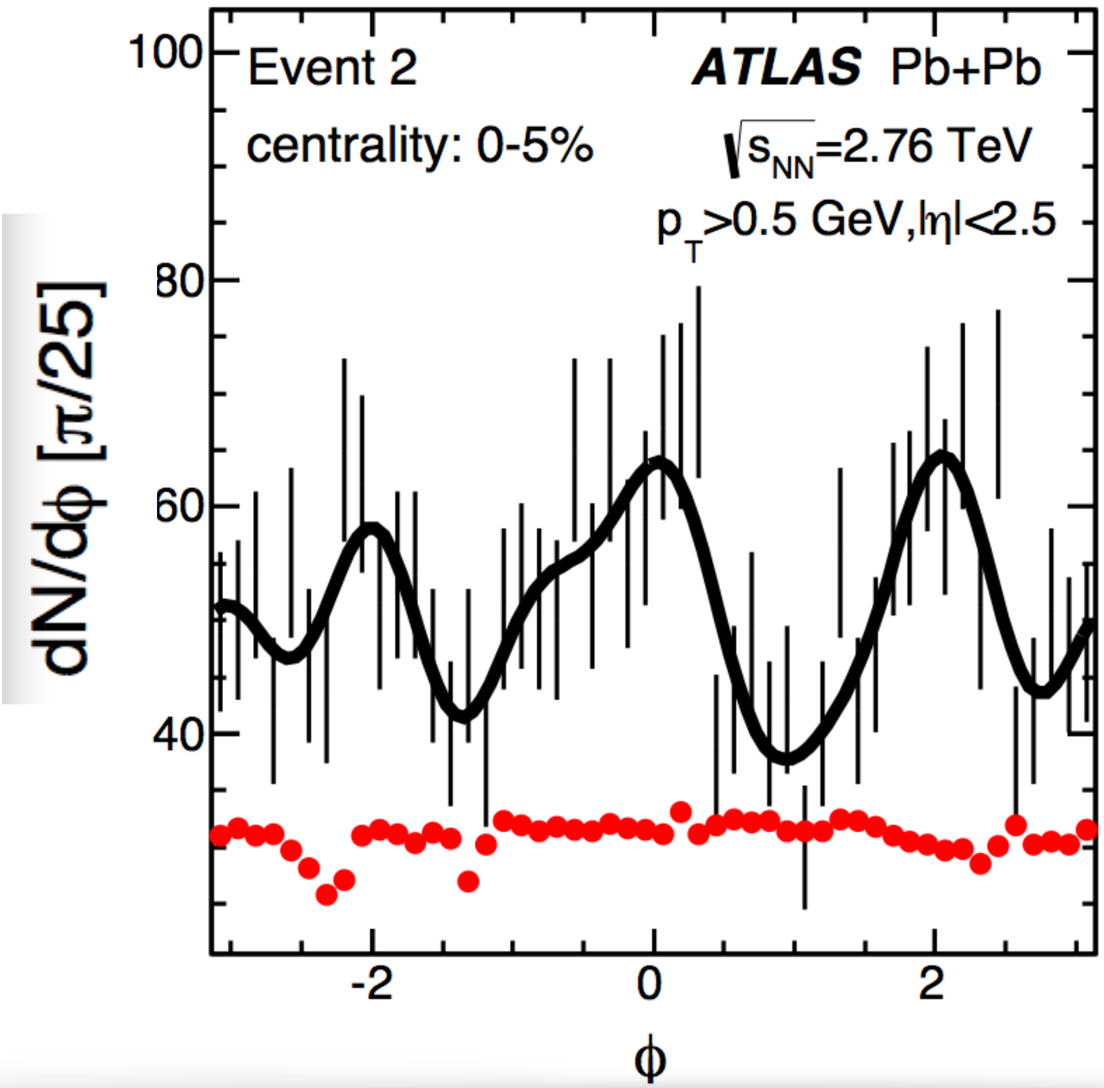

$$v_n(p_T)e^{in\Psi_n} = \frac{\int d\phi_p e^{in\phi_p} dN/(dy p_T dp_T d\phi_p)}{\int d\phi_p dN/(dy p_T dp_T d\phi_p)}$$

F.T. → $$N\left(1 + 2\sum_{n=1}^{\infty} v_n \cos(n(\phi_p - \Psi_n))\right)$$

- $\{v_n, \Psi_n\}$ captures the anisotropy in particle azimuthal momentum distribution

G. Aad *et al.* [ATLAS Collaboration], JHEP **1311**, 183 (2013)

Charged hadron v_n at the LHC

S. McDonald, C. Shen, F. Fillion-Gourdeau, S. Jeon and C. Gale, Phys. Rev. C 95, 064913 (2017)

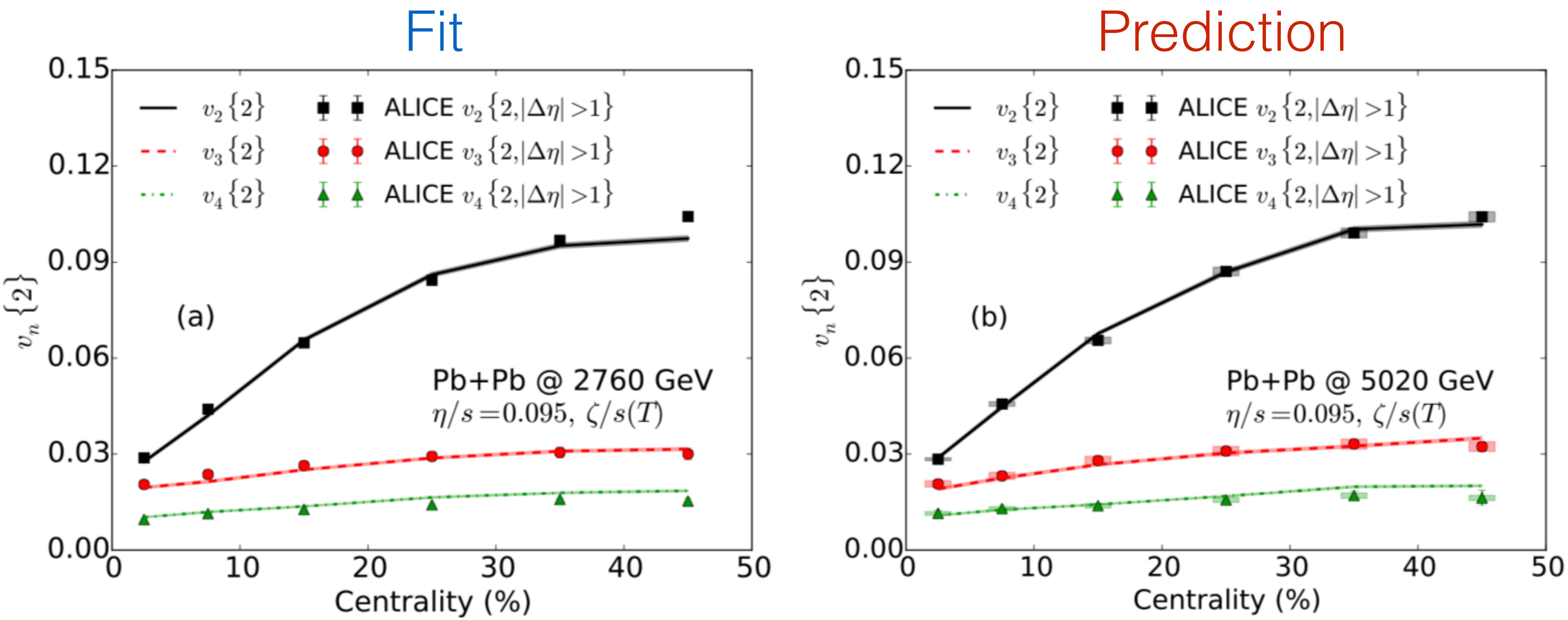

- Hydrodynamics can fit and <u>predict</u> anisotropic flow v_n
- The *conversion rate* of initial spatial eccentricity to final momentum anisotropy is controlled by the transport properties of the QGP

Extraction the QGP transport property

J. E. Bernhard, J. S. Moreland, S. A. Bass, J. Liu and U. Heinz, Phys. Rev. C 94, 024907 (2016)

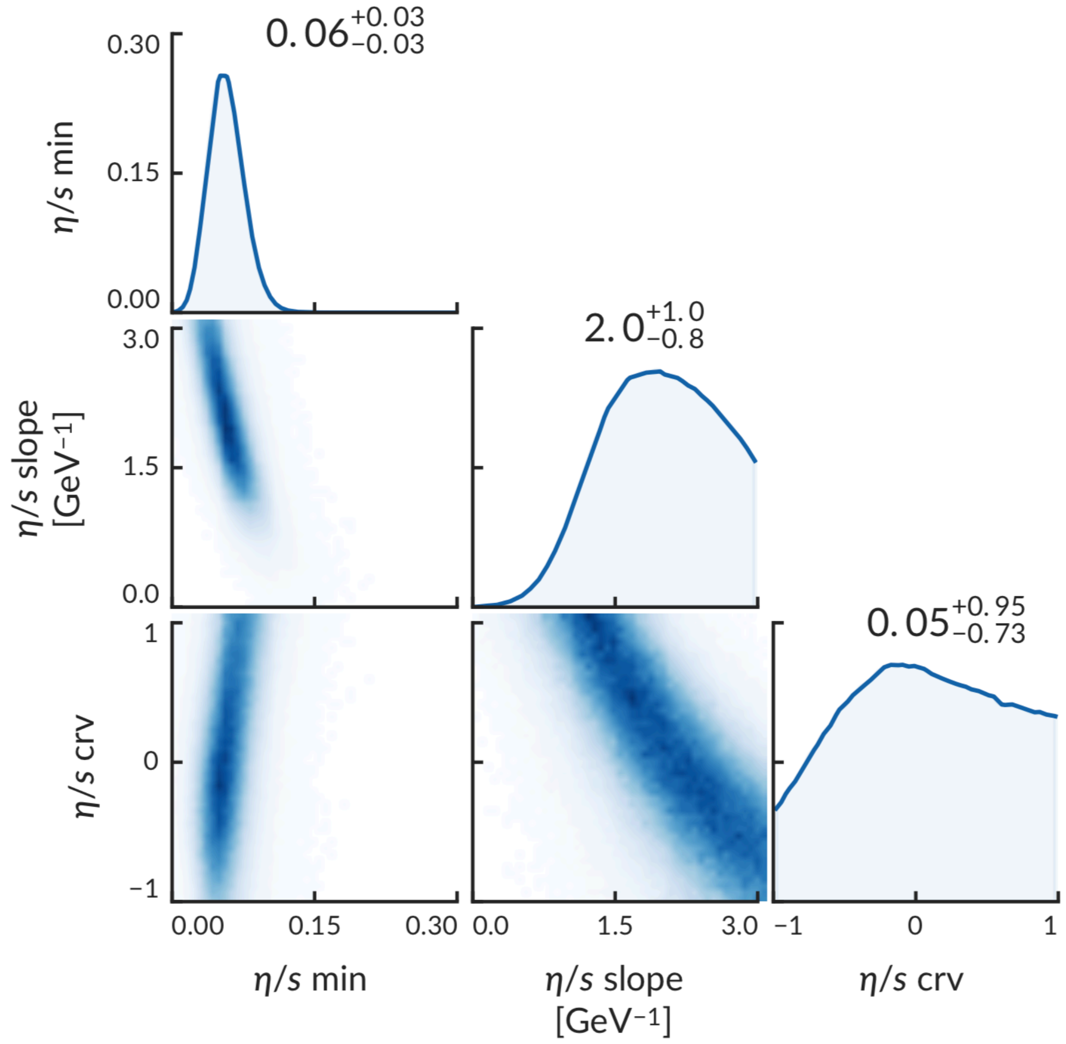

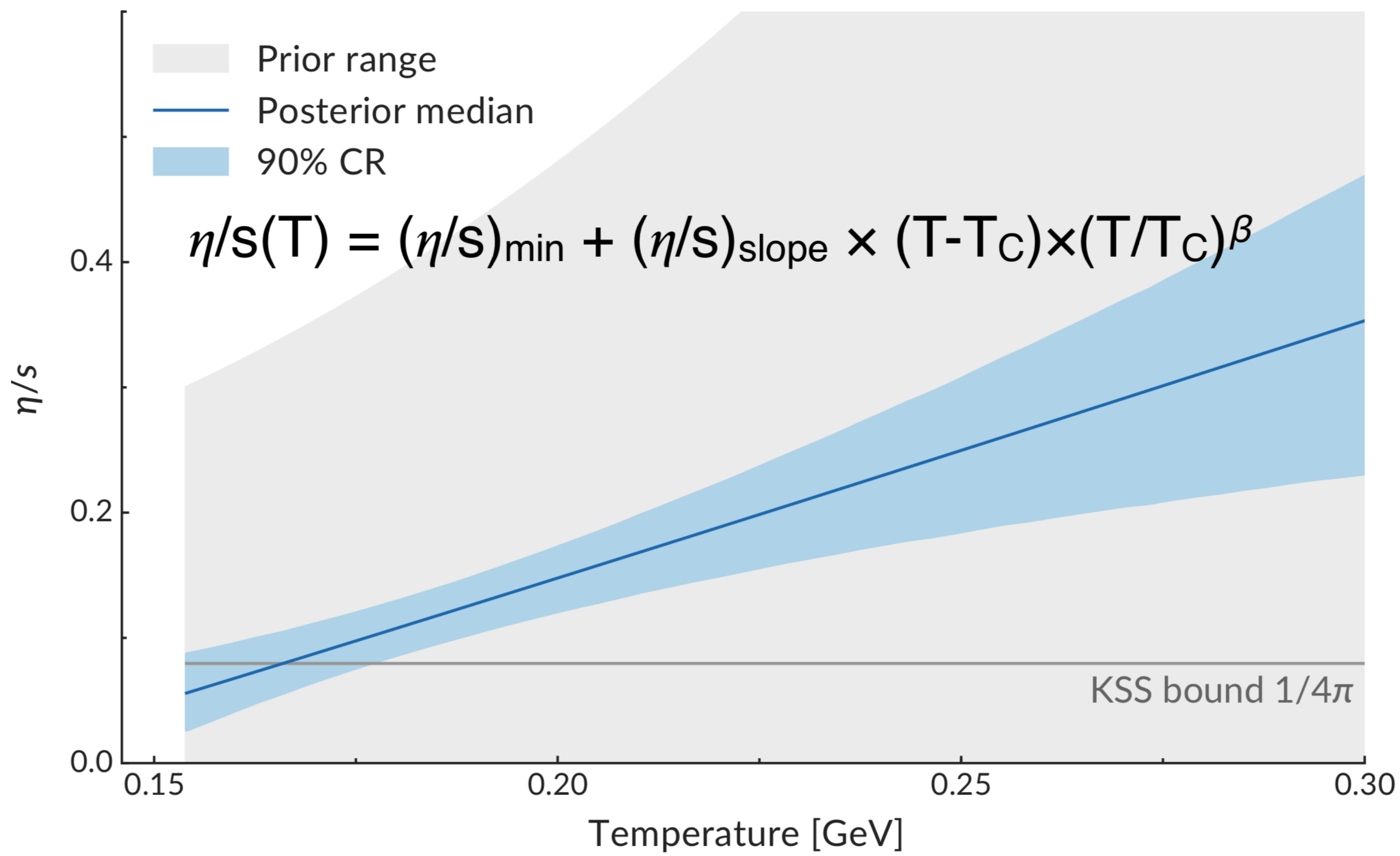

- Hydrodynamic framework is coupled with the Bayesian statistical analysis to provide the state-of-the-art extraction of the QGP shear viscosity

Universal hydrodynamic response

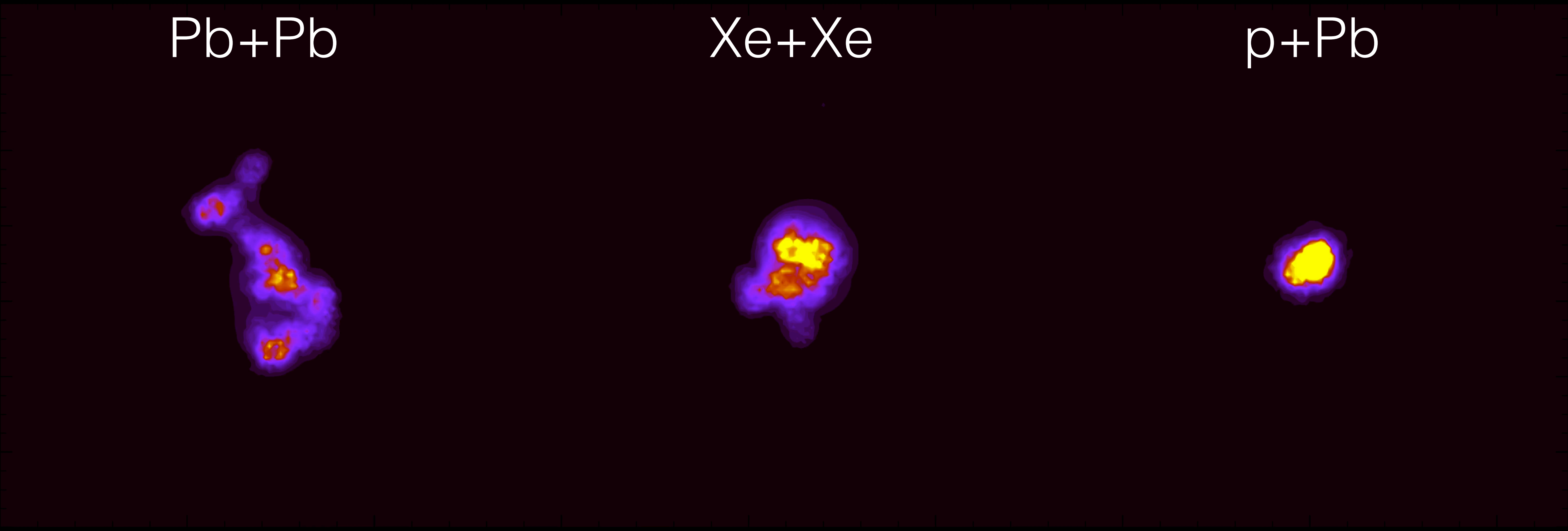

System size dependence of v_n

Bjoern Schenke, Chun Shen, and Prithwish Tribedy, in preparation

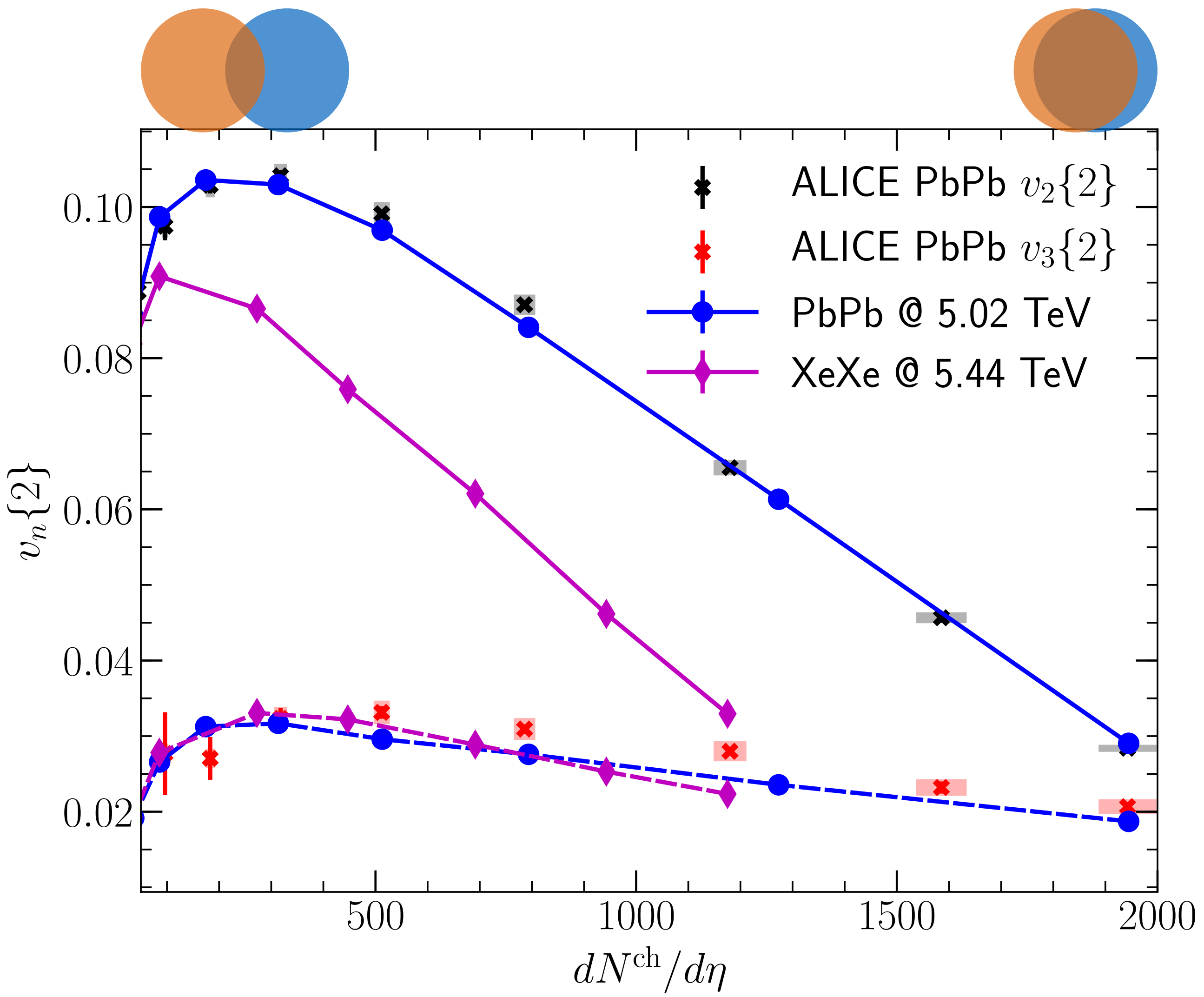

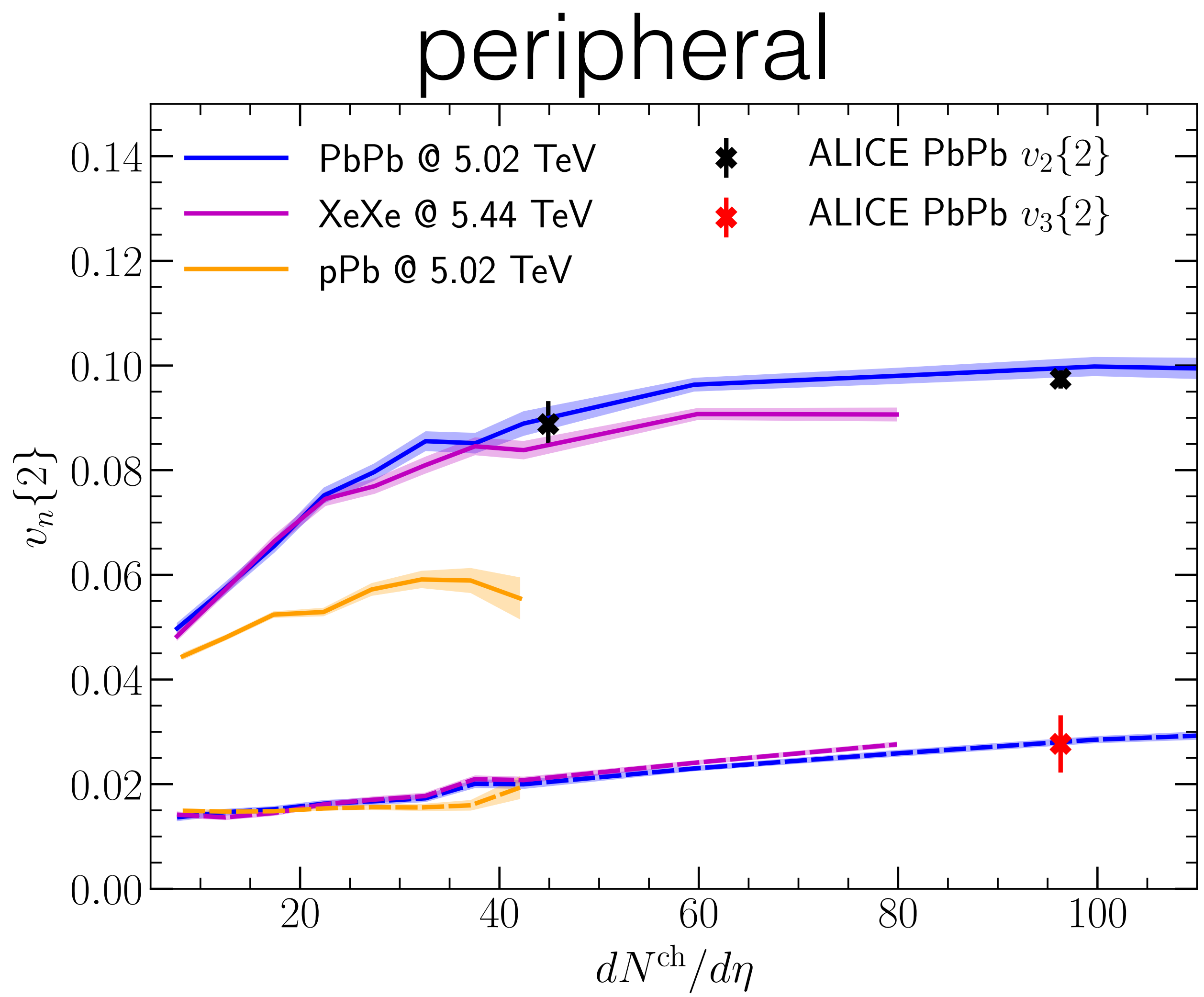

- The IP-Glasma + hydrodynamic framework can reproduce charged hadron $v_n\{2\}$ from central to peripheral collisions

Event-by-event fluctuation of v_n

Bjoern Schenke, Chun Shen, and Prithwish Tribedy, in preparation

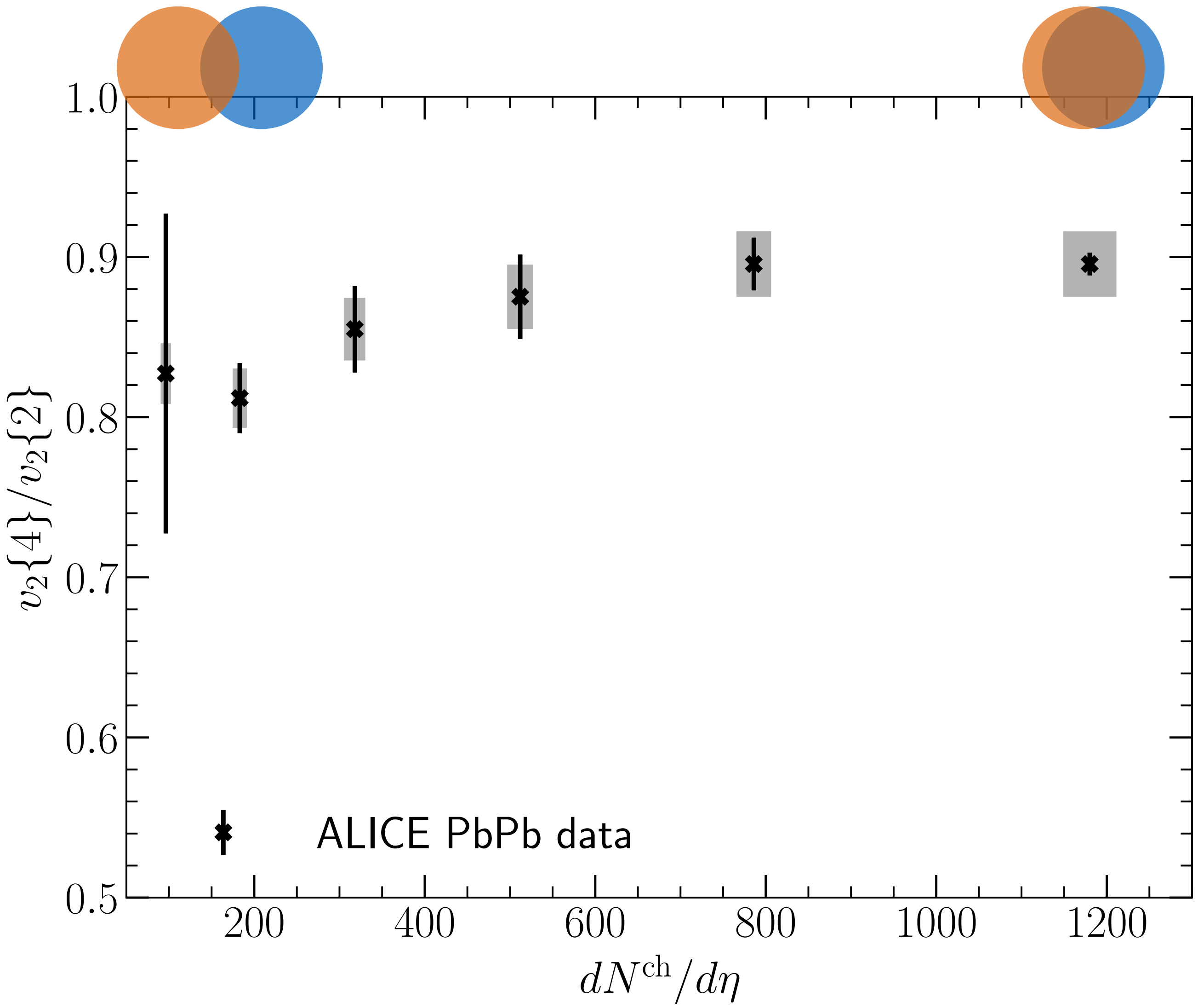

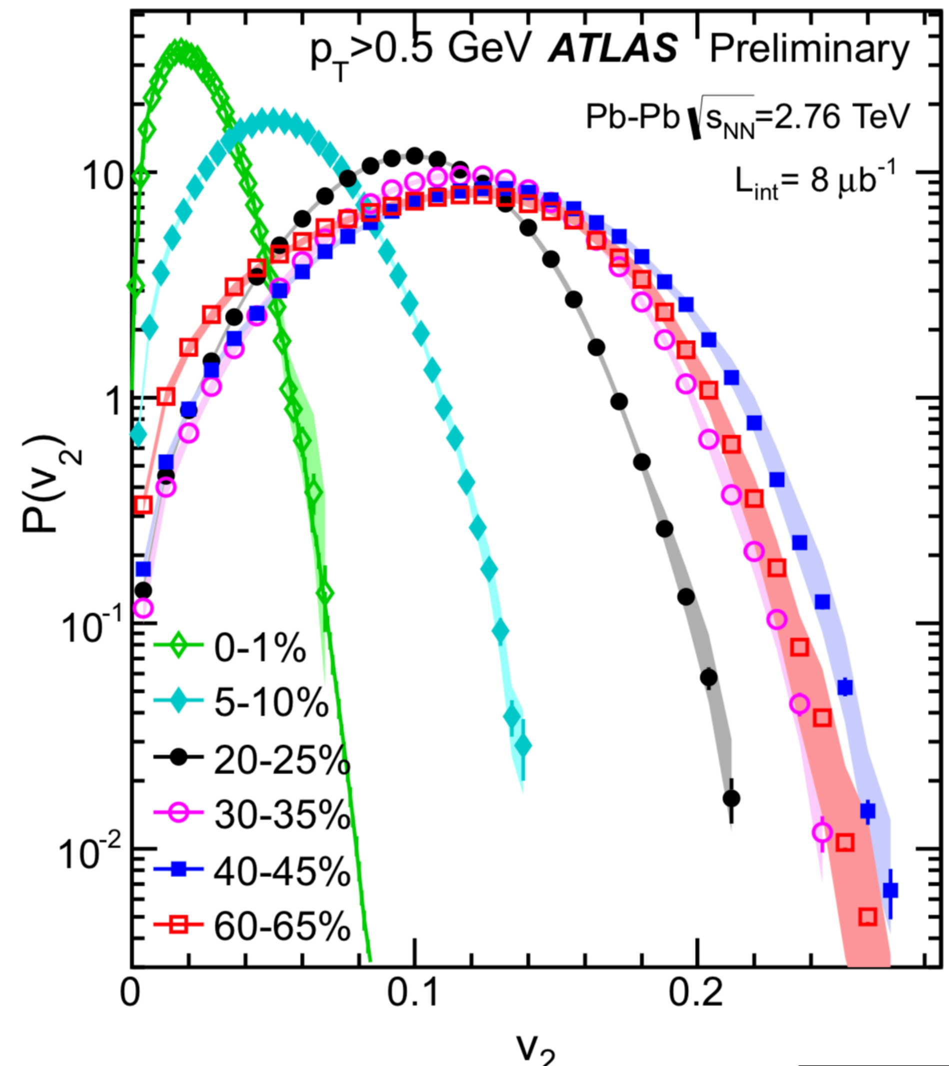

ATLAS-CONF -2012-114

- The ratio of $v_2\{4\}/v_2\{2\}$ measures the variance of the v_2 fluctuations

$$\frac{v_2\{4\}}{v_2\{2\}} \longrightarrow \sqrt{\frac{1-(\sigma^2/\bar{v}_2^2)}{1+(\sigma^2/\bar{v}_2^2)}}$$

Event-by-event fluctuation of v_n

Bjoern Schenke, Chun Shen, and Prithwish Tribedy, in preparation

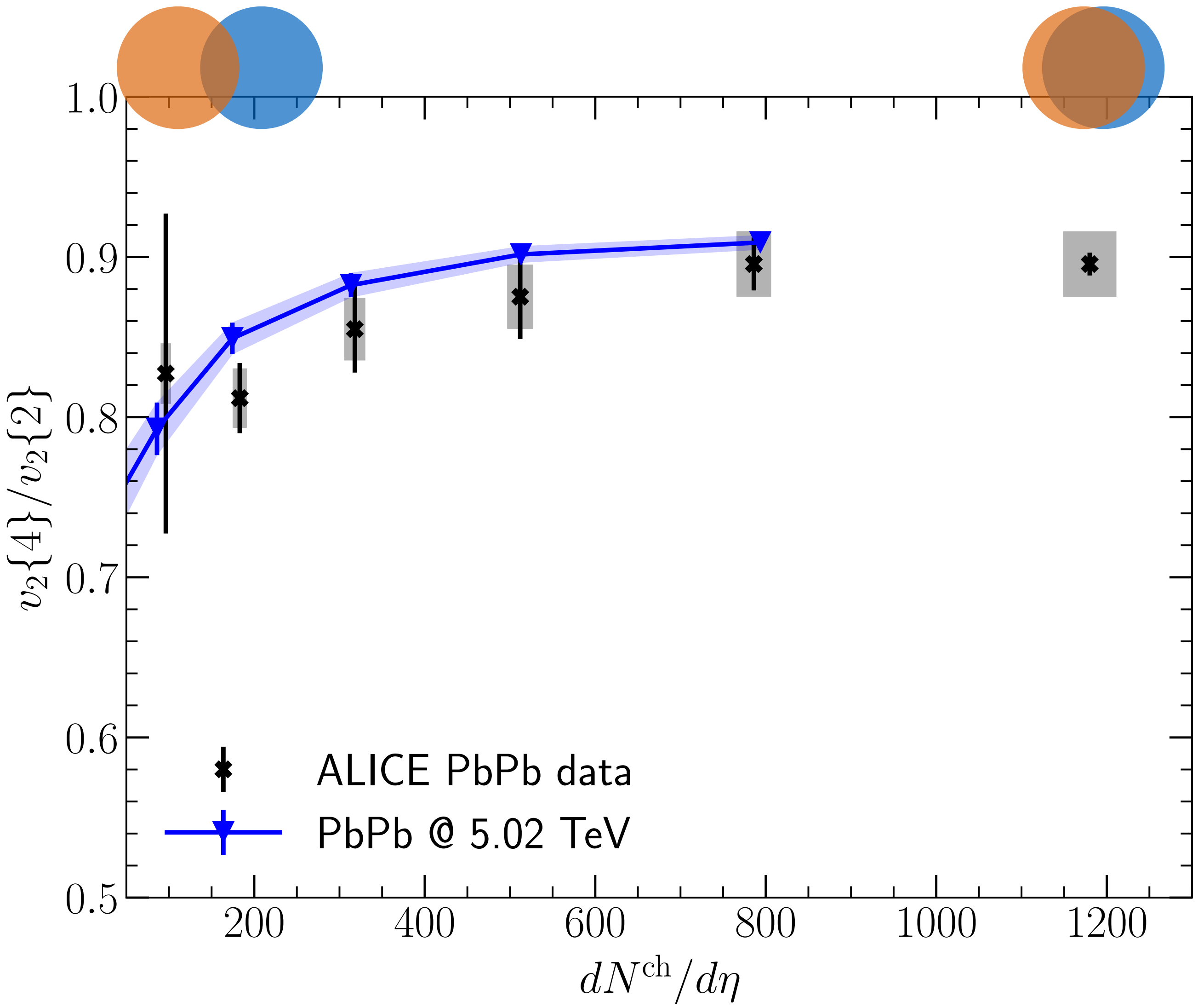

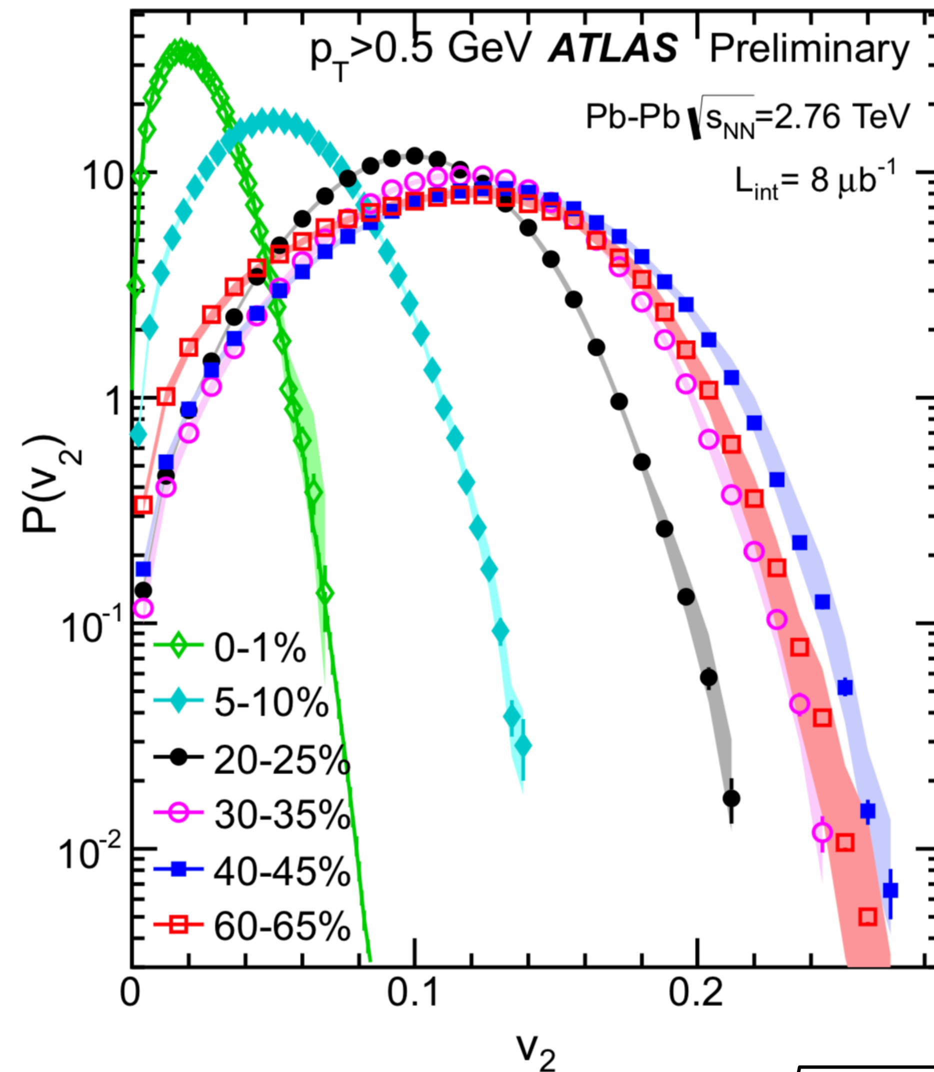

ATLAS-CONF -2012-114

- The ratio of $v_2\{4\}/v_2\{2\}$ measures the variance of the v_2 fluctuations $\frac{v_2\{4\}}{v_2\{2\}} \longrightarrow \sqrt{\frac{1-(\sigma^2/\bar{v}_2^2)}{1+(\sigma^2/\bar{v}_2^2)}}$
- The IP-Glasma initial condition captures the v_2 fluctuations from central to peripheral centralities

Event-by-event fluctuation of v_n

Bjoern Schenke, Chun Shen, and Prithwish Tribedy, in preparation

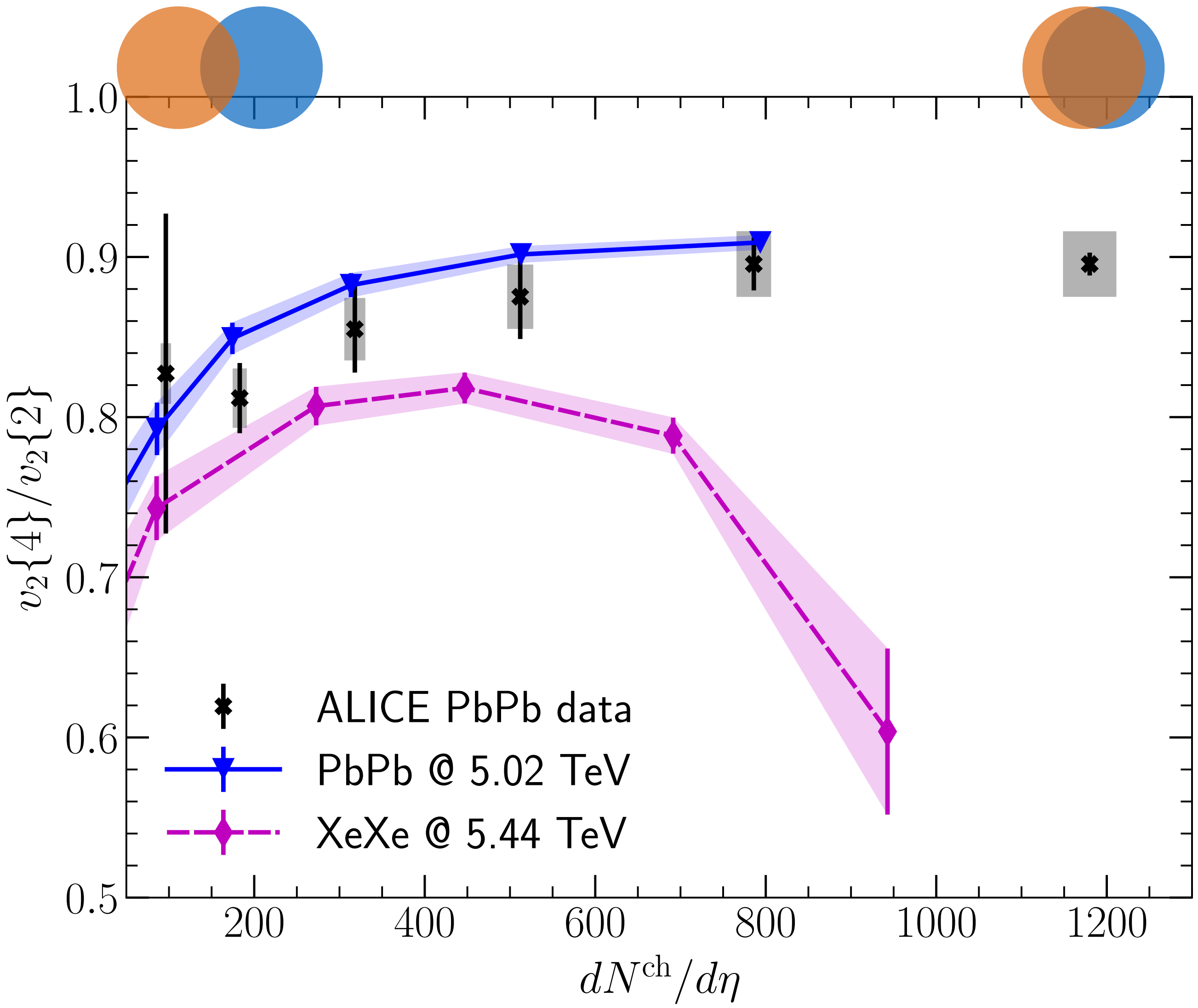

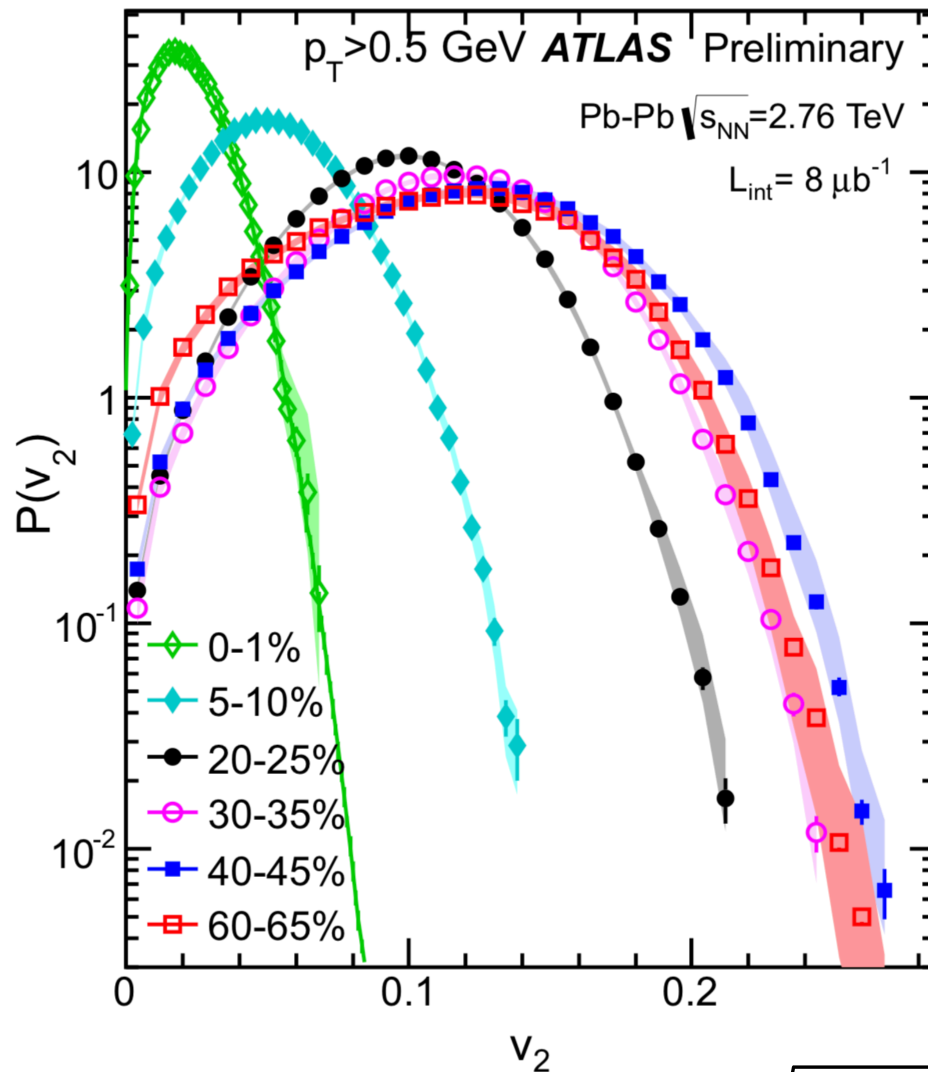

ATLAS-CONF -2012-114

- The ratio of $v_2\{4\}/v_2\{2\}$ measures the variance of the v_2 fluctuations $$\frac{v_2\{4\}}{v_2\{2\}} \longrightarrow \sqrt{\frac{1-(\sigma^2/\bar{v}_2^2)}{1+(\sigma^2/\bar{v}_2^2)}}$$
- The IP-Glasma initial condition captures the v_2 fluctuations from central to peripheral centralities

Event-by-event fluctuation of v_n

Bjoern Schenke, Chun Shen, and Prithwish Tribedy, in preparation

central

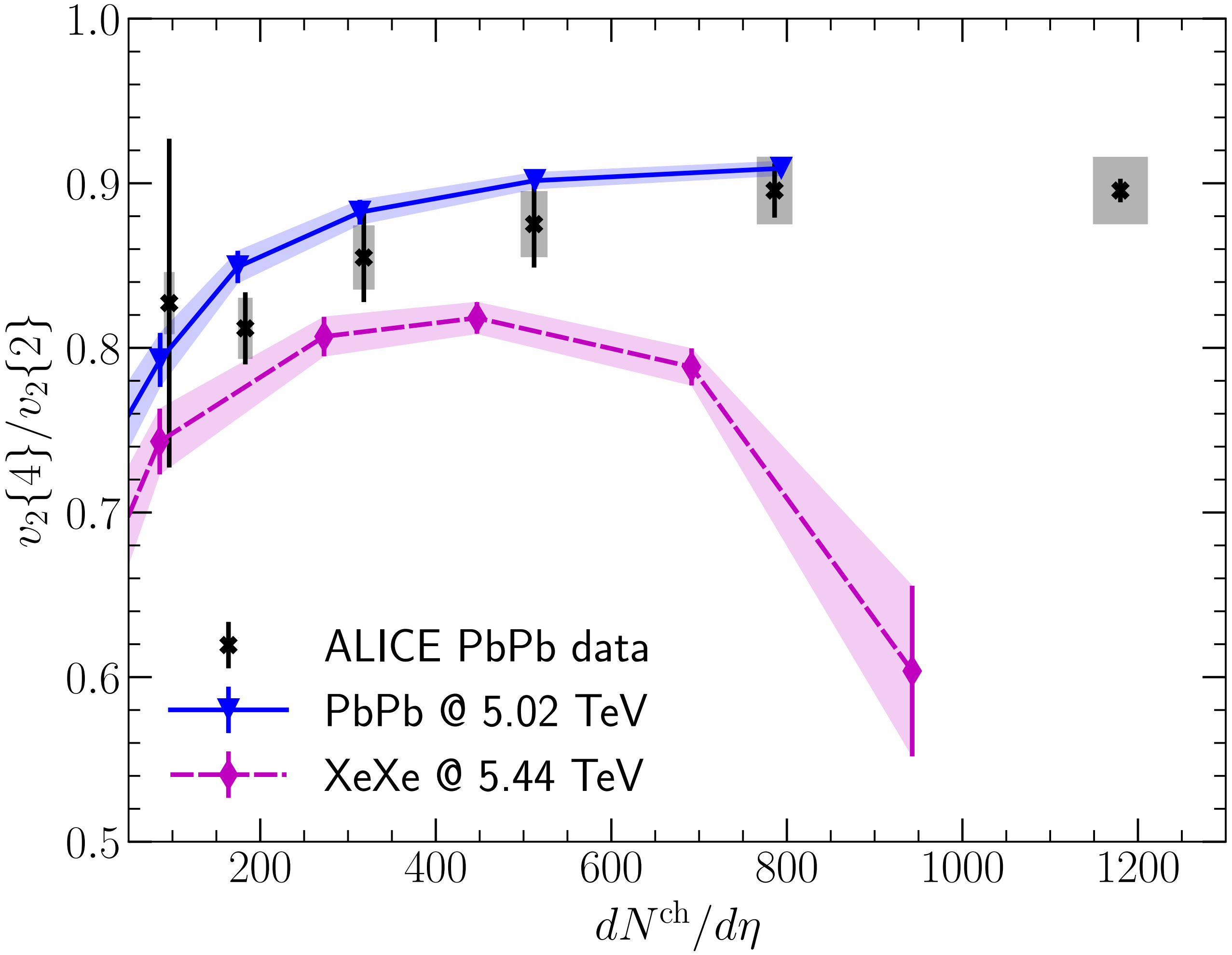

peripheral

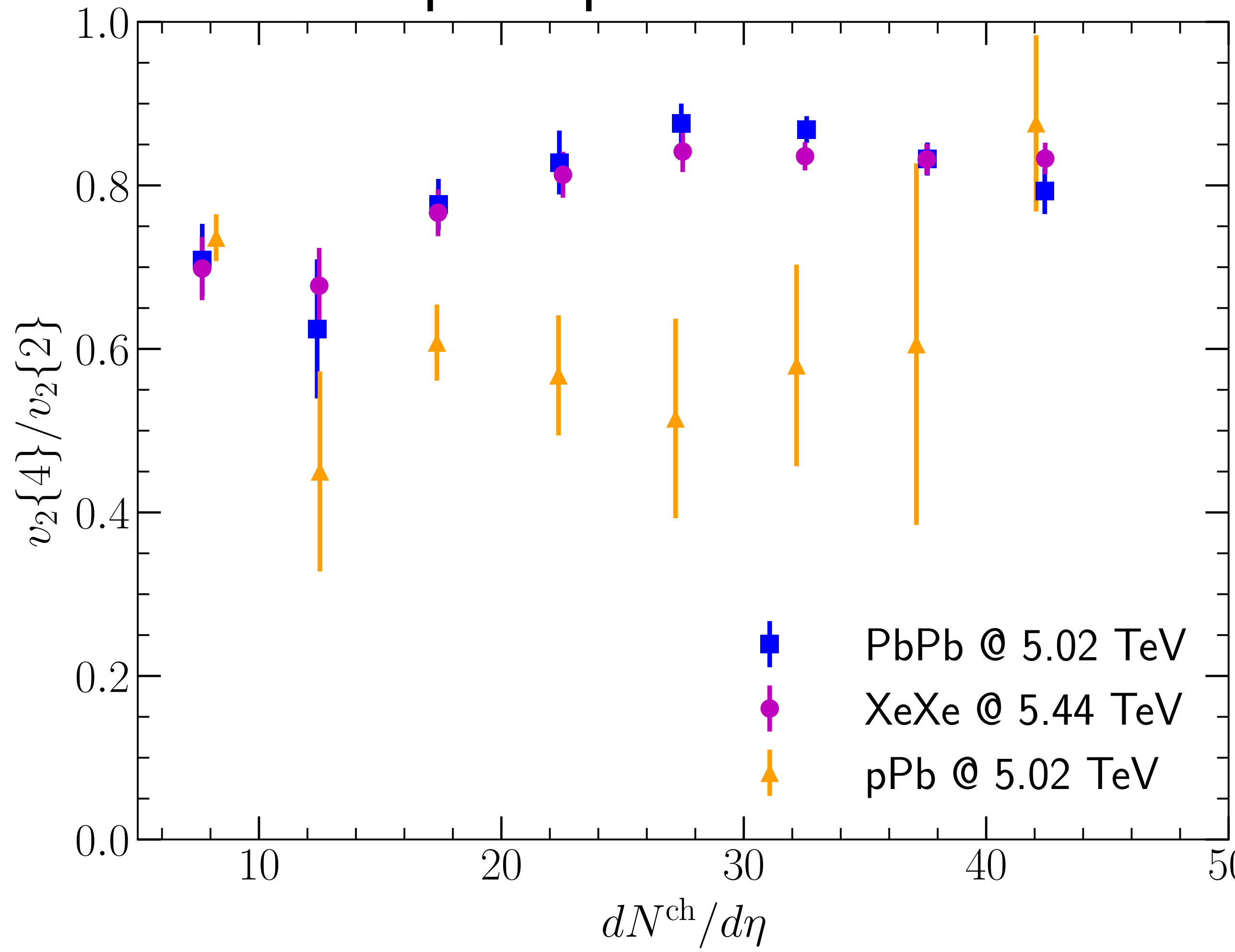

- The ratio of $v_2\{4\}/v_2\{2\}$ measures the variance of the v_2 fluctuations $\frac{v_2\{4\}}{v_2\{2\}} \longrightarrow \sqrt{\frac{1-(\sigma^2/\bar{v}_2^2)}{1+(\sigma^2/\bar{v}_2^2)}}$
- A larger v_2 fluctuation is in pPb collisions compared to the larger XeXe and PbPb collisions at a same $dN^{\mathrm{ch}}/d\eta$

Non-Gaussianity of v_n fluctuations

Bjoern Schenke, Chun Shen, and Prithwish Tribedy, in preparation

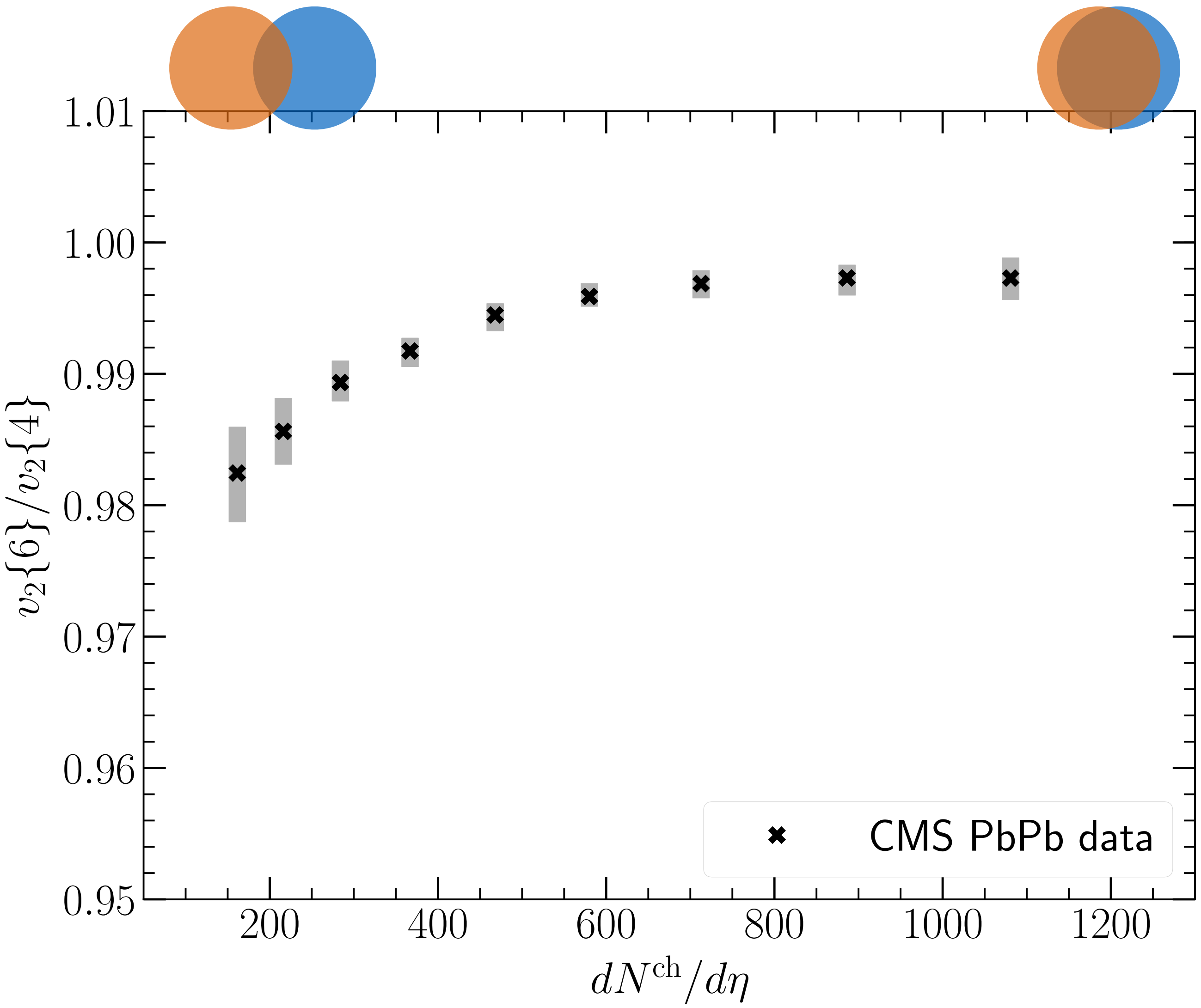

The Bessel-Gaussian fluctuation gives $v_2\{4\} = v_2\{6\}$

G. Giacalone, L. Yan, J. Noronha-Hostler and J. Y. Ollitrault, Phys. Rev. C 95, 014913 (2017)

More generally,

$$v_2\{4\} \simeq \bar{v}_2 + \frac{\sigma_y^2 - \sigma_x^2}{2\bar{v}_2} - \frac{s_1 + s_2}{(\bar{v}_2)^2},$$

$$v_2\{6\} \simeq \bar{v}_2 + \frac{\sigma_y^2 - \sigma_x^2}{2\bar{v}_2} - \frac{\frac{2}{3}s_1 + s_2}{(\bar{v}_2)^2},$$

$$s_1 \equiv \langle (v_x - \bar{v}_2)^3 \rangle,$$
$$s_2 \equiv \langle (v_x - \bar{v}_2) v_y^2 \rangle.$$

- The difference between $v_2\{4\}$ and $v_2\{6\}$ raises from the skewness of the v_2 distribution

Non-Gaussianity of v_n fluctuations

Bjoern Schenke, Chun Shen, and Prithwish Tribedy, in preparation

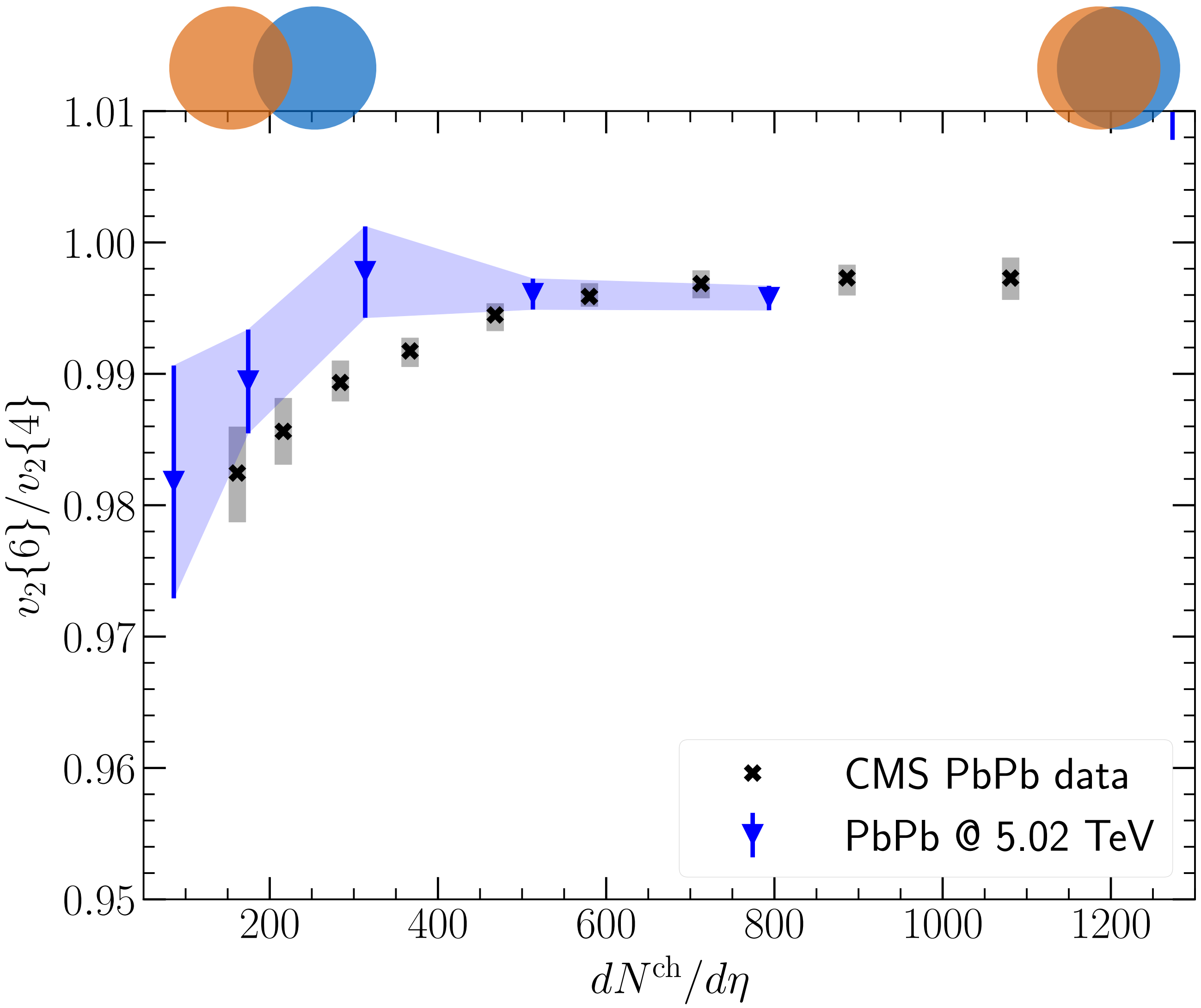

The Bessel-Gaussian fluctuation gives $v_2\{4\} = v_2\{6\}$

G. Giacalone, L. Yan, J. Noronha-Hostler and J. Y. Ollitrault, Phys. Rev. C 95, 014913 (2017)

More generally,

$$v_2\{4\} \simeq \bar{v}_2 + \frac{\sigma_y^2 - \sigma_x^2}{2\bar{v}_2} - \frac{s_1 + s_2}{(\bar{v}_2)^2},$$

$$v_2\{6\} \simeq \bar{v}_2 + \frac{\sigma_y^2 - \sigma_x^2}{2\bar{v}_2} - \frac{\frac{2}{3}s_1 + s_2}{(\bar{v}_2)^2},$$

$$s_1 \equiv \langle (v_x - \bar{v}_2)^3 \rangle,$$
$$s_2 \equiv \langle (v_x - \bar{v}_2) v_y^2 \rangle.$$

- The difference between $v_2\{4\}$ and $v_2\{6\}$ raises from the skewness of the v_2 distribution
- The IP-Glasma + hydrodynamic framework reproduces the $v_2\{6\}/v_2\{4\}$ ratio for PbPb collisions

Non-Gaussianity of v_n fluctuations

Bjoern Schenke, Chun Shen, and Prithwish Tribedy, in preparation

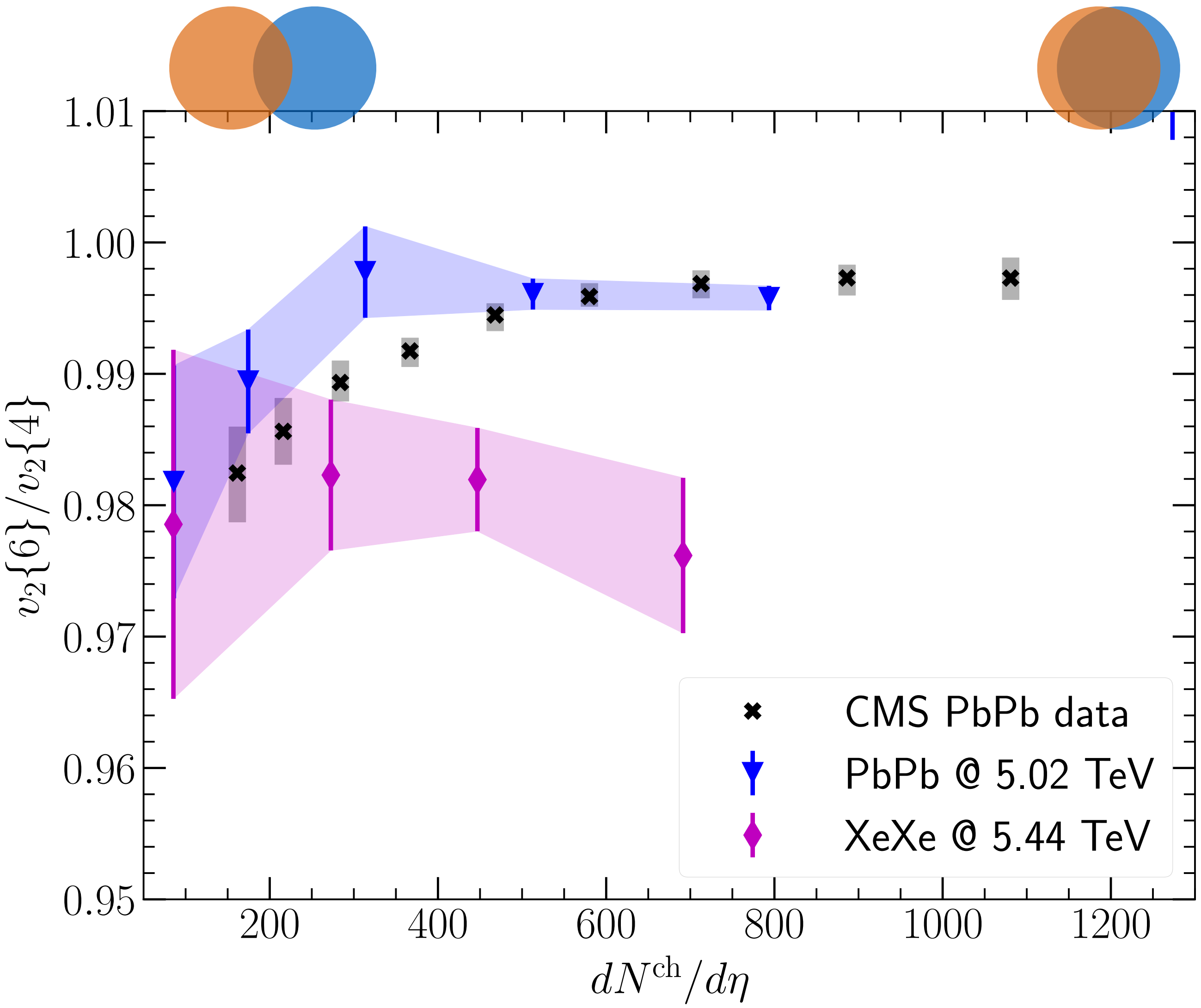

The Bessel-Gaussian fluctuation gives $v_2\{4\} = v_2\{6\}$

G. Giacalone, L. Yan, J. Noronha-Hostler and J. Y. Ollitrault, Phys. Rev. C 95, 014913 (2017)

More generally,

$$v_2\{4\} \simeq \bar{v}_2 + \frac{\sigma_y^2 - \sigma_x^2}{2\bar{v}_2} - \frac{s_1 + s_2}{(\bar{v}_2)^2},$$

$$v_2\{6\} \simeq \bar{v}_2 + \frac{\sigma_y^2 - \sigma_x^2}{2\bar{v}_2} - \frac{\frac{2}{3}s_1 + s_2}{(\bar{v}_2)^2},$$

$$s_1 \equiv \langle (v_x - \bar{v}_2)^3 \rangle,$$
$$s_2 \equiv \langle (v_x - \bar{v}_2) v_y^2 \rangle.$$

- The difference between $v_2\{4\}$ and $v_2\{6\}$ raises from the skewness of the v_2 distribution
- The IP-Glasma + hydrodynamic framework reproduces the $v_2\{6\}/v_2\{4\}$ ratio for PbPb collisions

Non-Gaussianity of v_n fluctuations

Bjoern Schenke, Chun Shen, and Prithwish Tribedy, in preparation

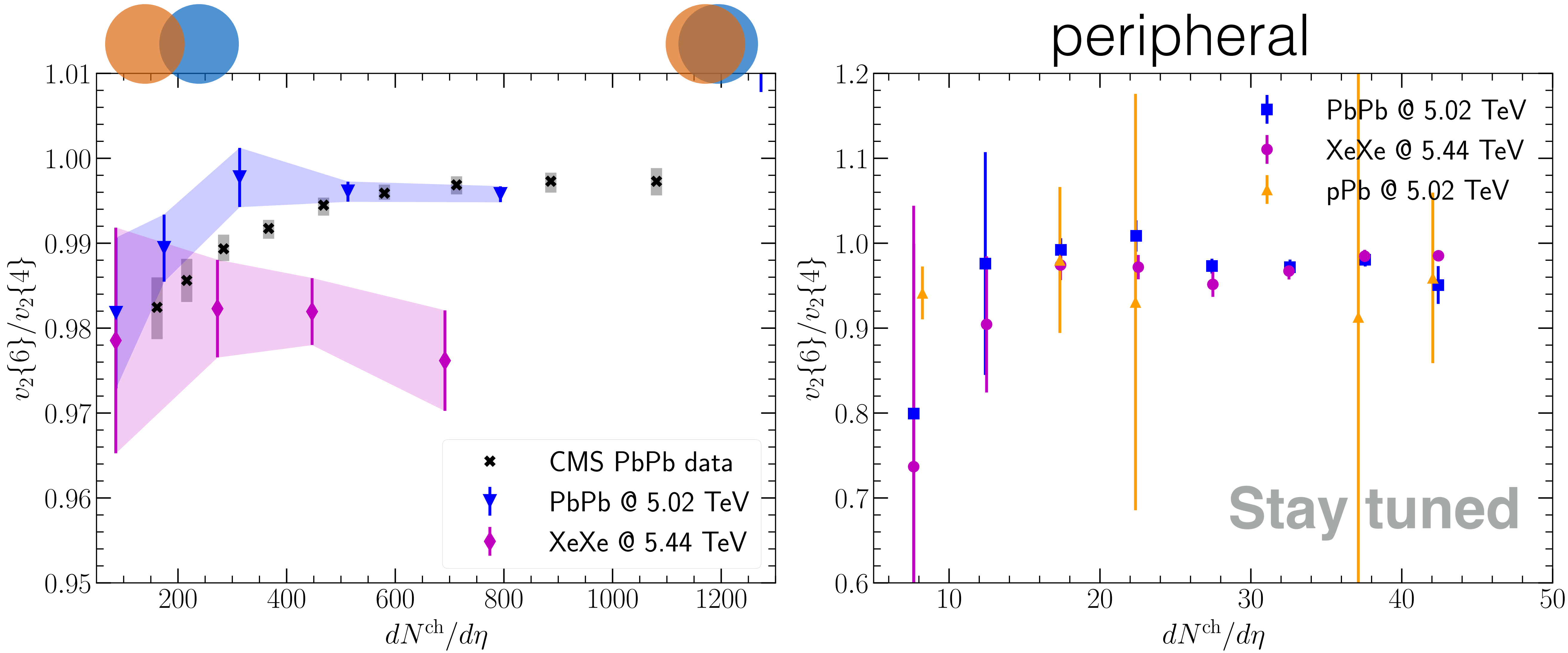

- The difference between $v_2\{4\}$ and $v_2\{6\}$ raises from the skewness of the v_2 distribution
- More statistics is needed for comparisons among p+Pb, Xe+Xe, and Pb+Pb collisions at small $dN^{ch}/d\eta$

Exploring the phases of QCD

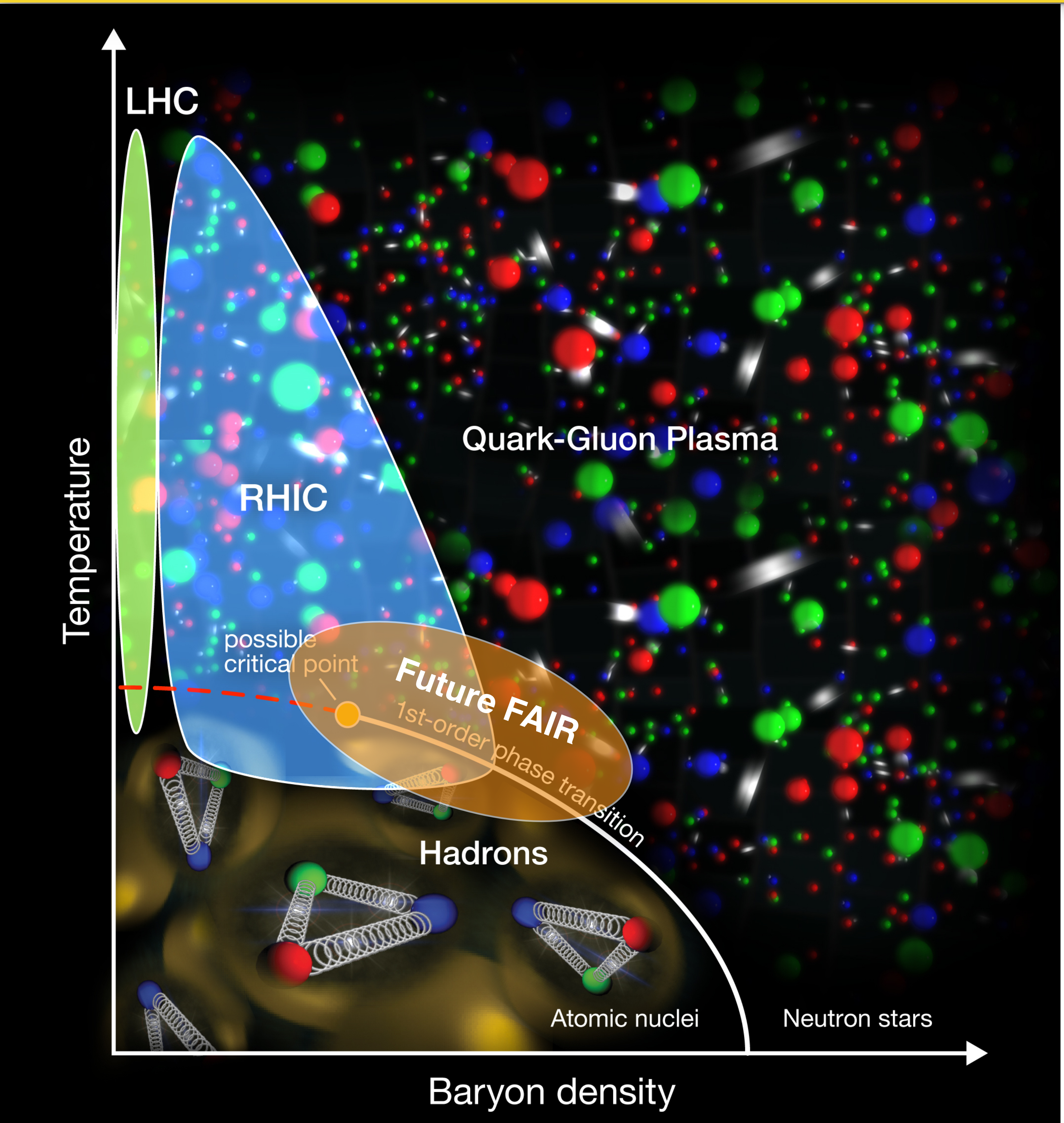

- Event-by-event fluctuating initial conditions and pre-equilibrium evolution
- (3+1)-d dissipative hydrodynamics with conserved charge currents
- Detailed microscopic description for hadronic phase

When to start hydrodynamics?

C. Shen and B. Schenke, arXiv:1710.00881 [nucl-th].

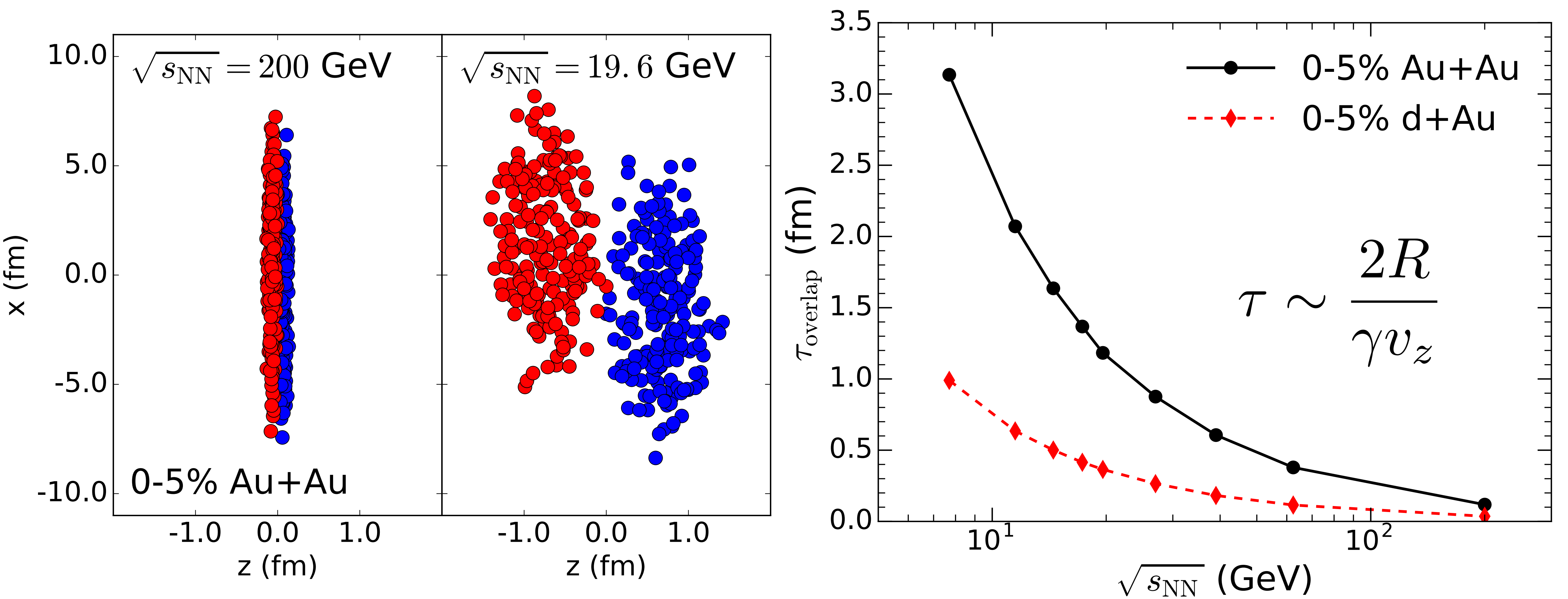

- Nuclei overlapping time is large at low collision energy
- Pre-equilibrium dynamics can play an important role

Go beyond the Bjorken approximation

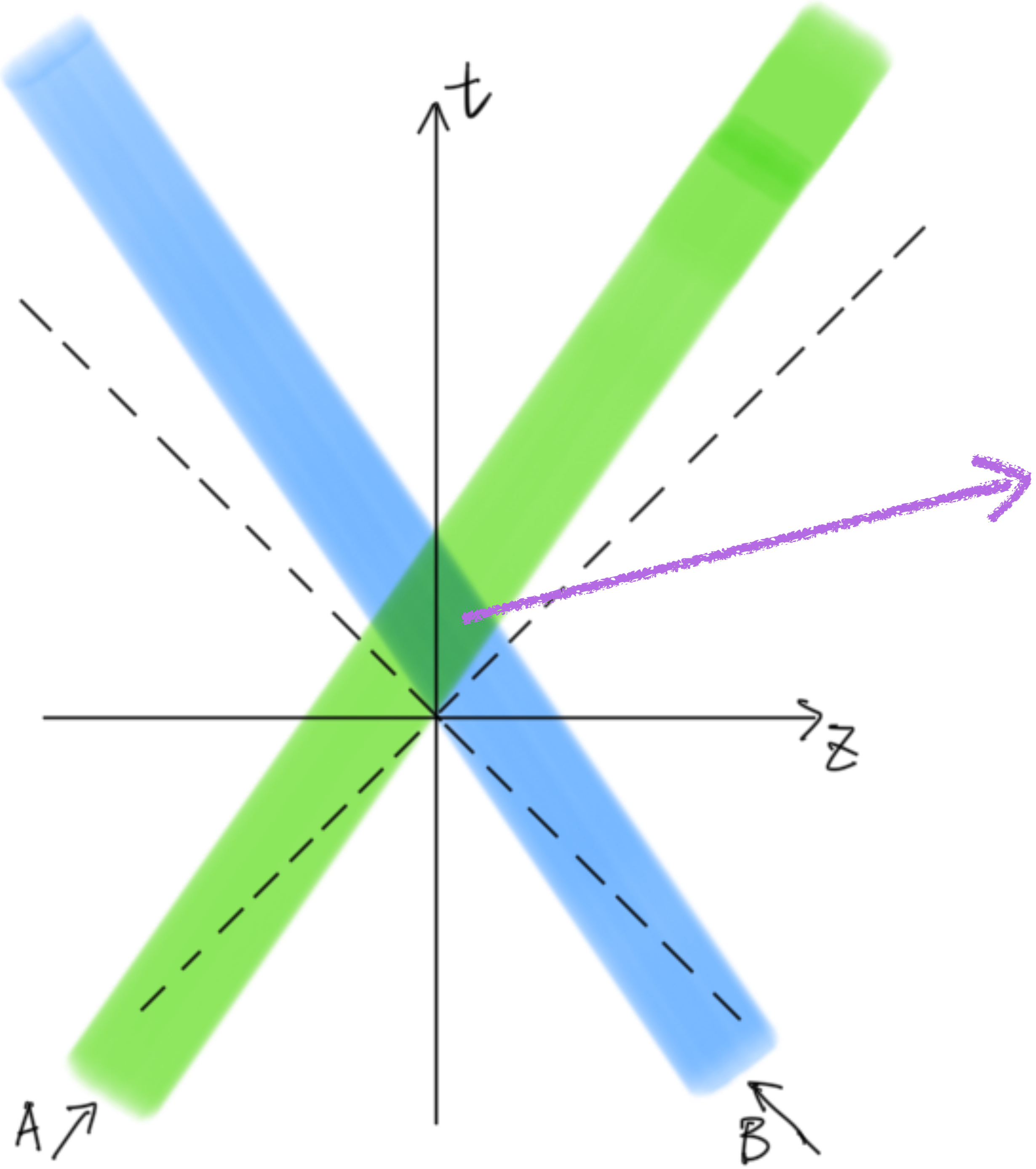

- The finite widths of the colliding nuclei are taken into account

The interaction zone is not point like

$$y \neq \eta_s$$

need full 3D **spatial** and **momentum** information

The 3D MC-Glauber model

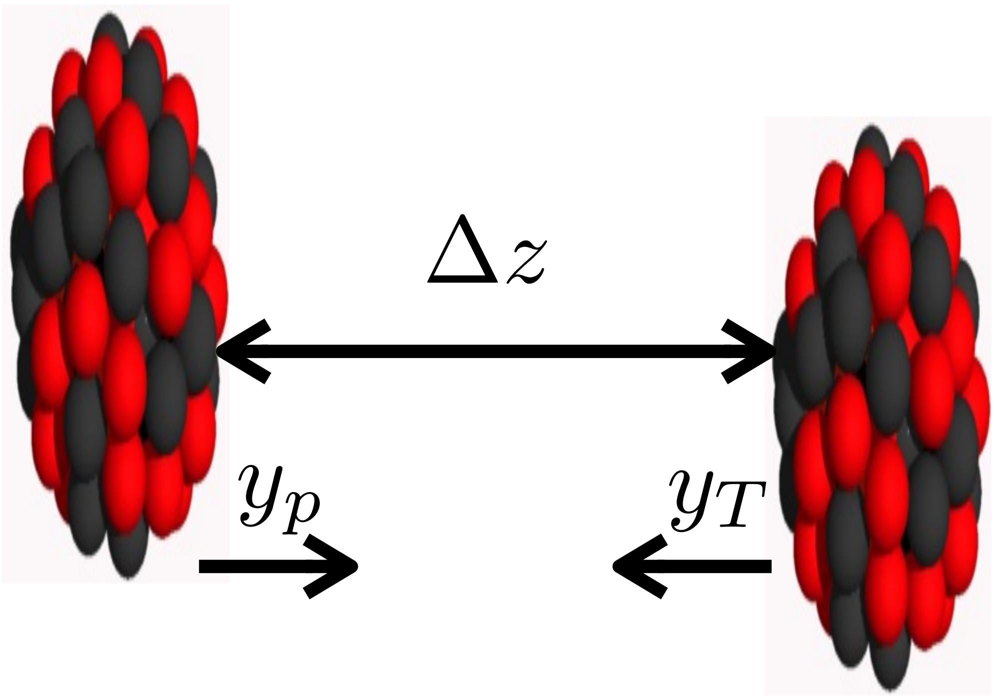

- Collision time and 3D spatial position are determined for every binary collision

The 3D MC-Glauber model

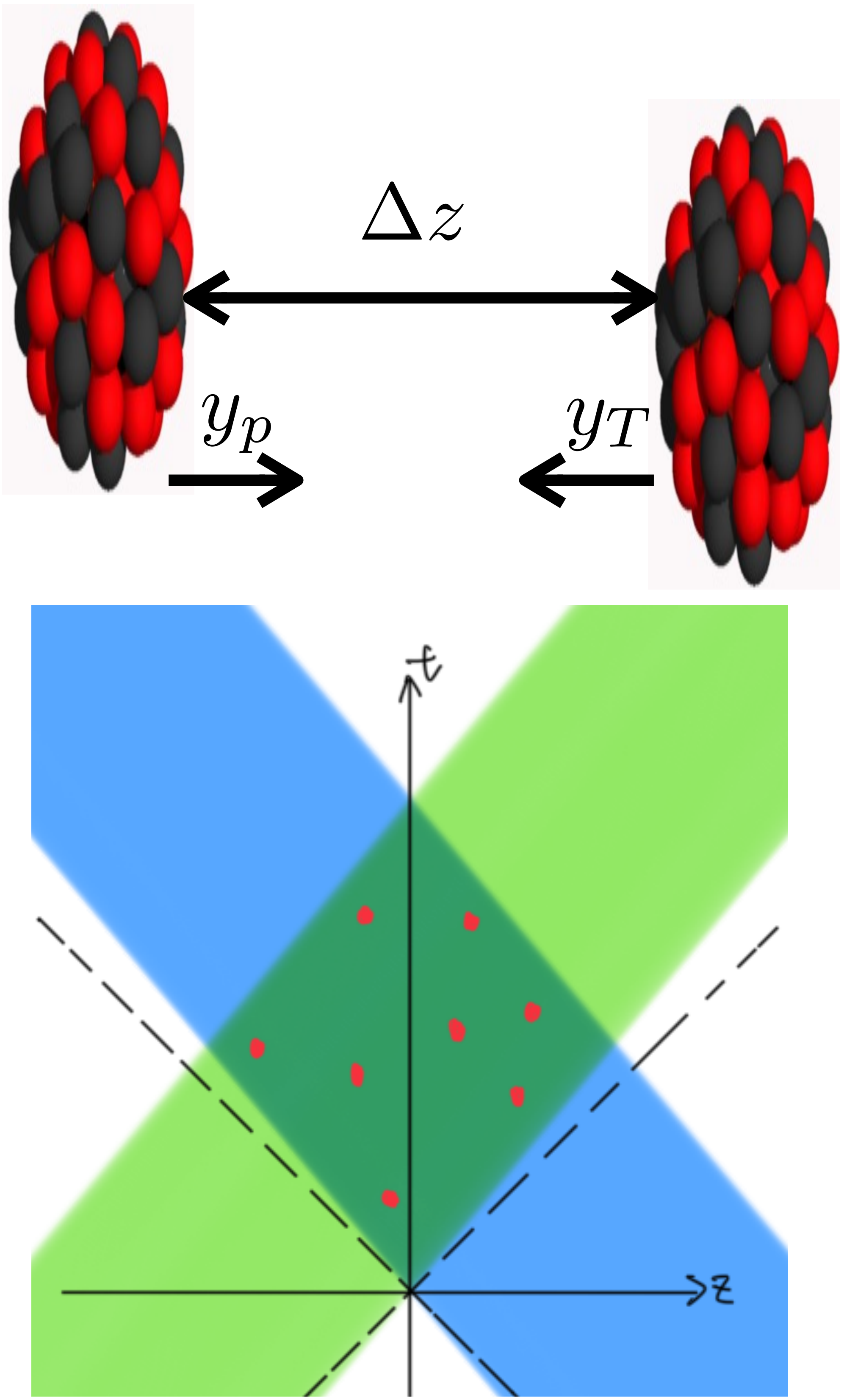

- Collision time and 3D spatial position are determined for every binary collision
- QCD strings are randomly produced from collision points

The 3D MC-Glauber model

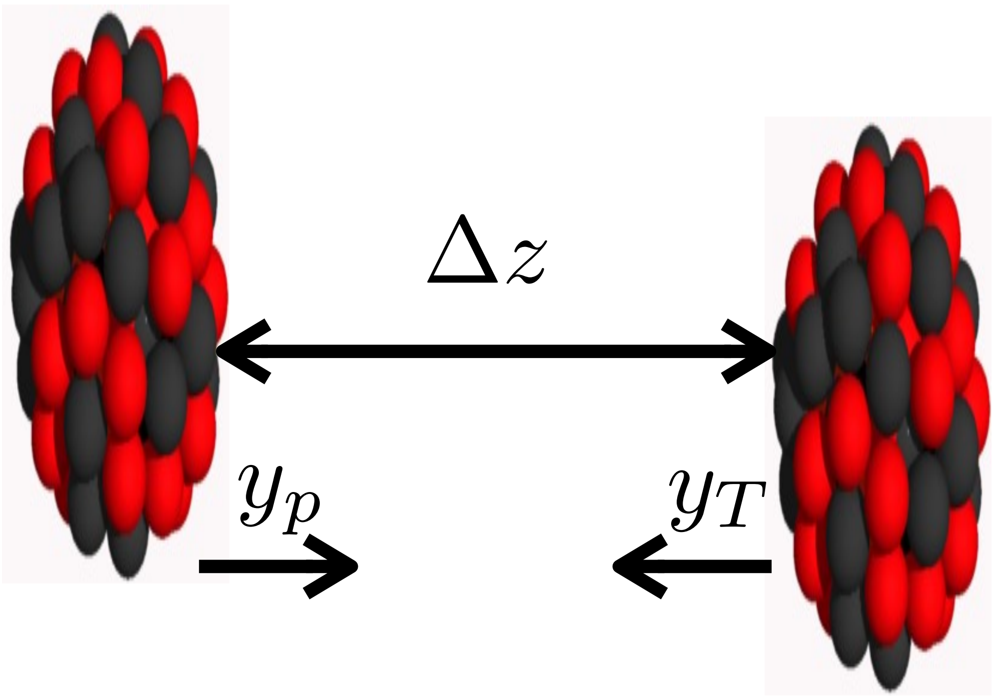

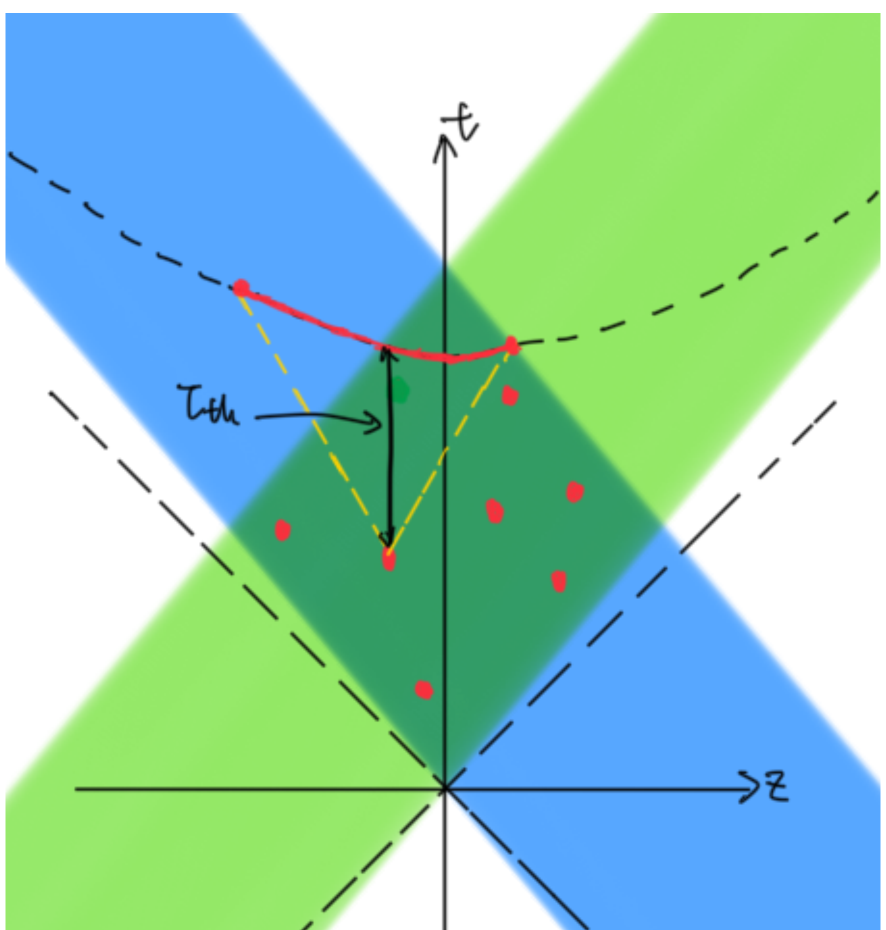

- Collision time and 3D spatial position are determined for every binary collision
- QCD strings are randomly produced from collision points

A. Bialas, A. Bzdak and V. Koch, arXiv:1608.07041 [hep-ph]

- These strings are decelerated with a constant string tension $\sigma = 1 GeV/fm$ before thermalized to medium

String space-time distribution

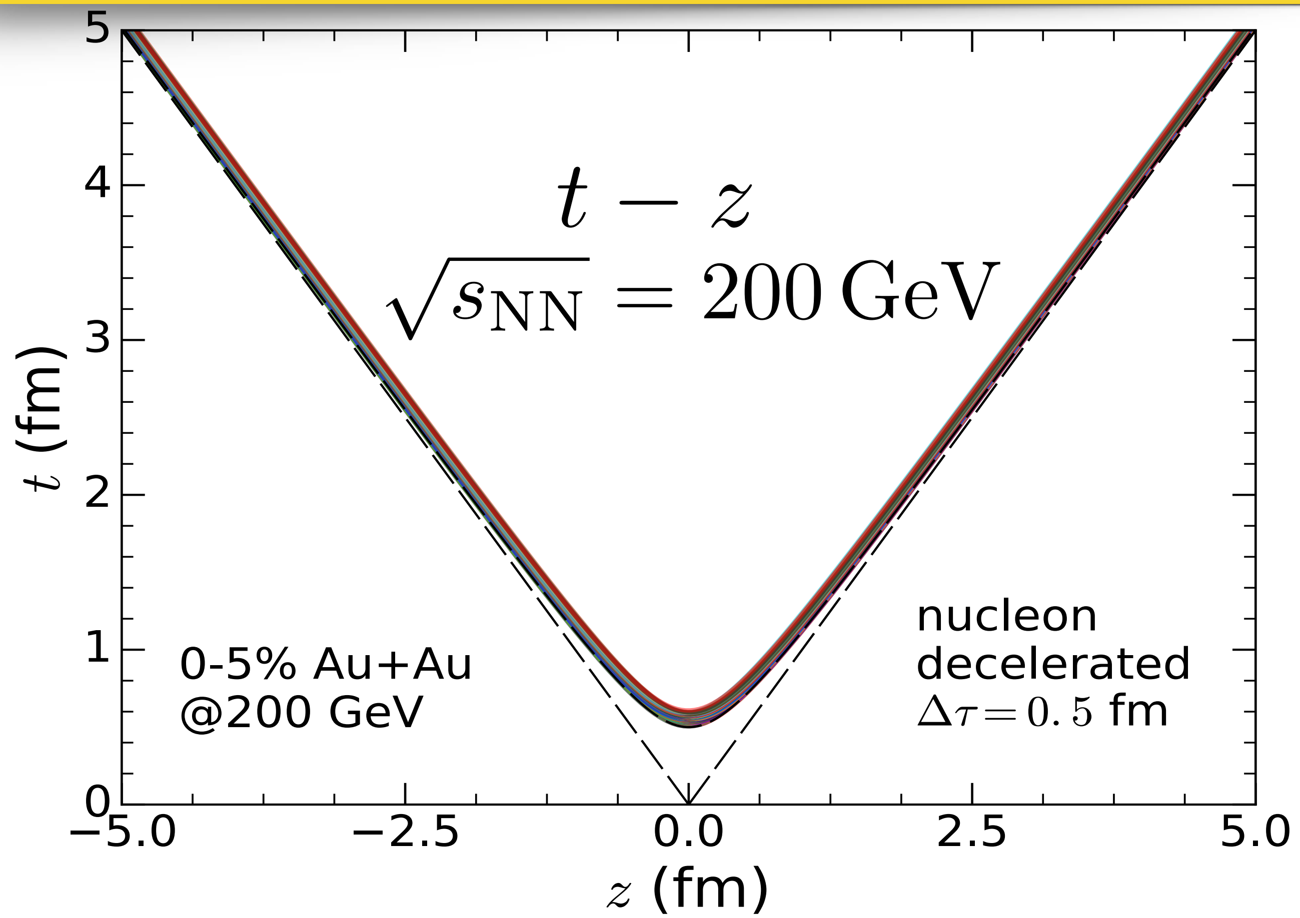

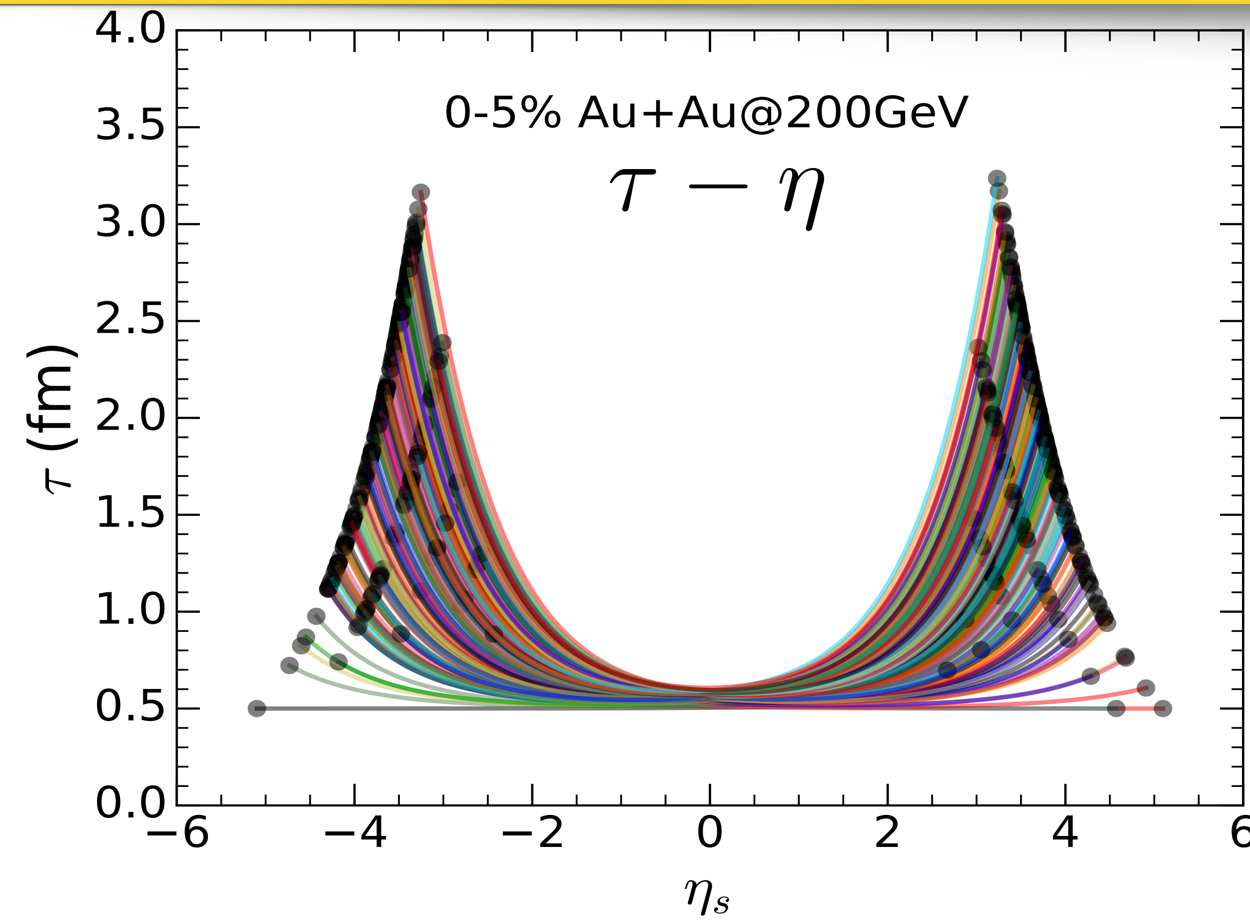

String space-time distribution

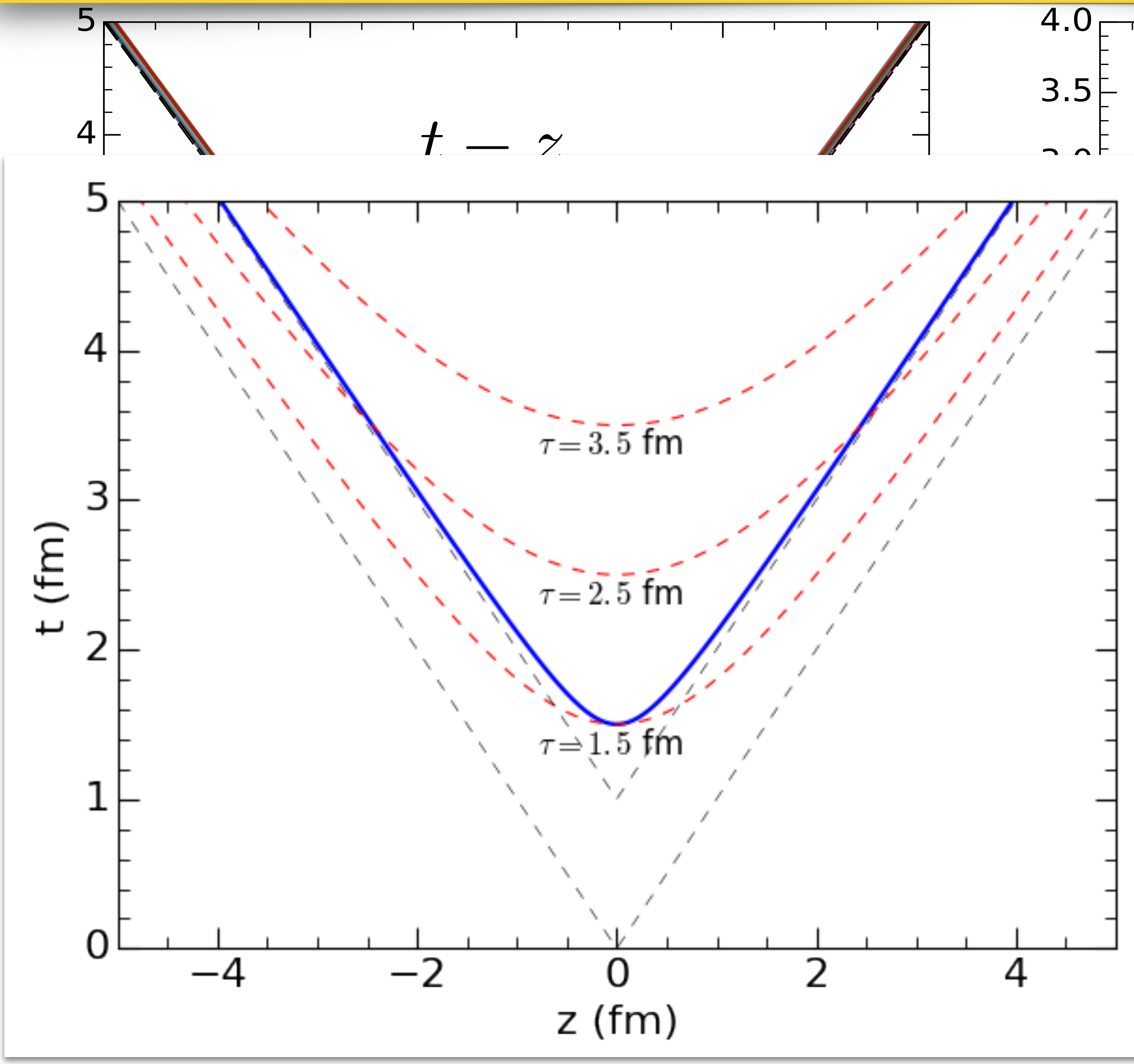

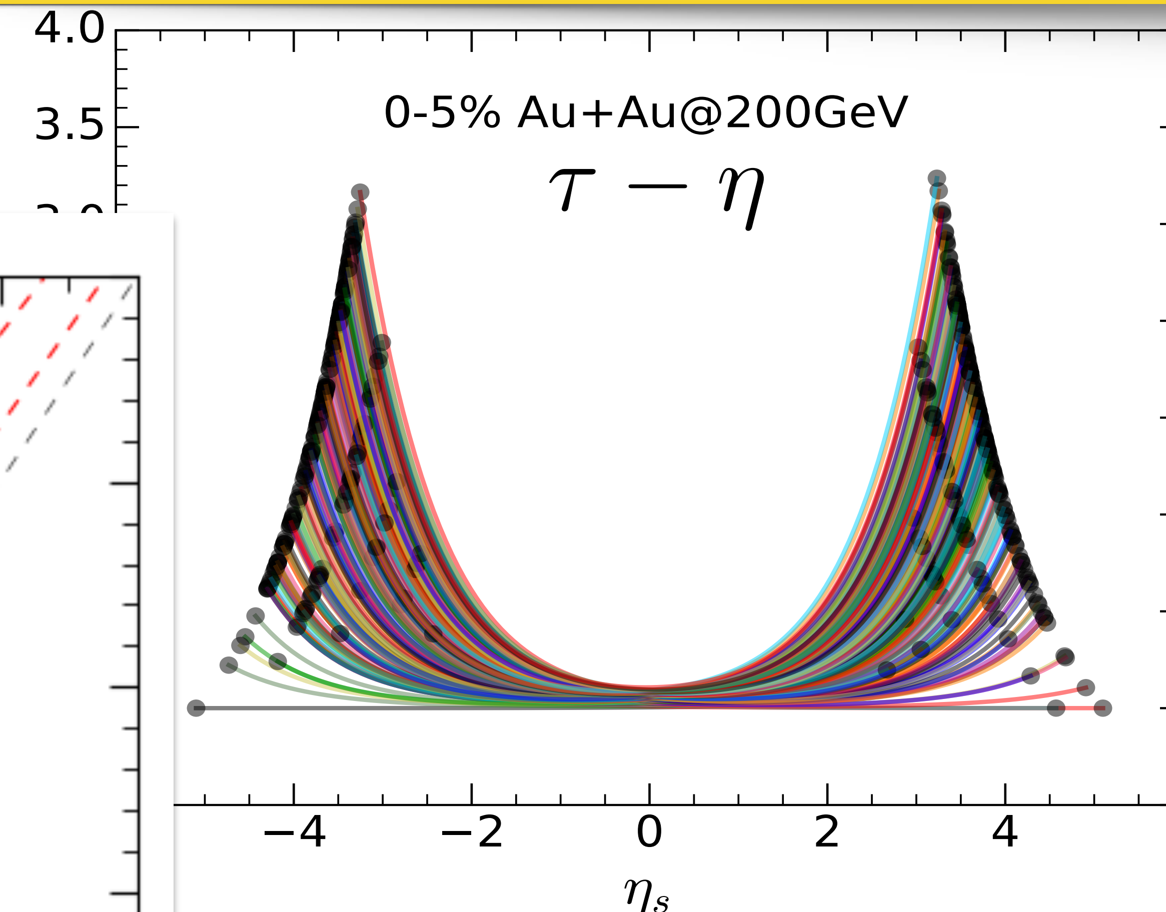

String space-time distribution

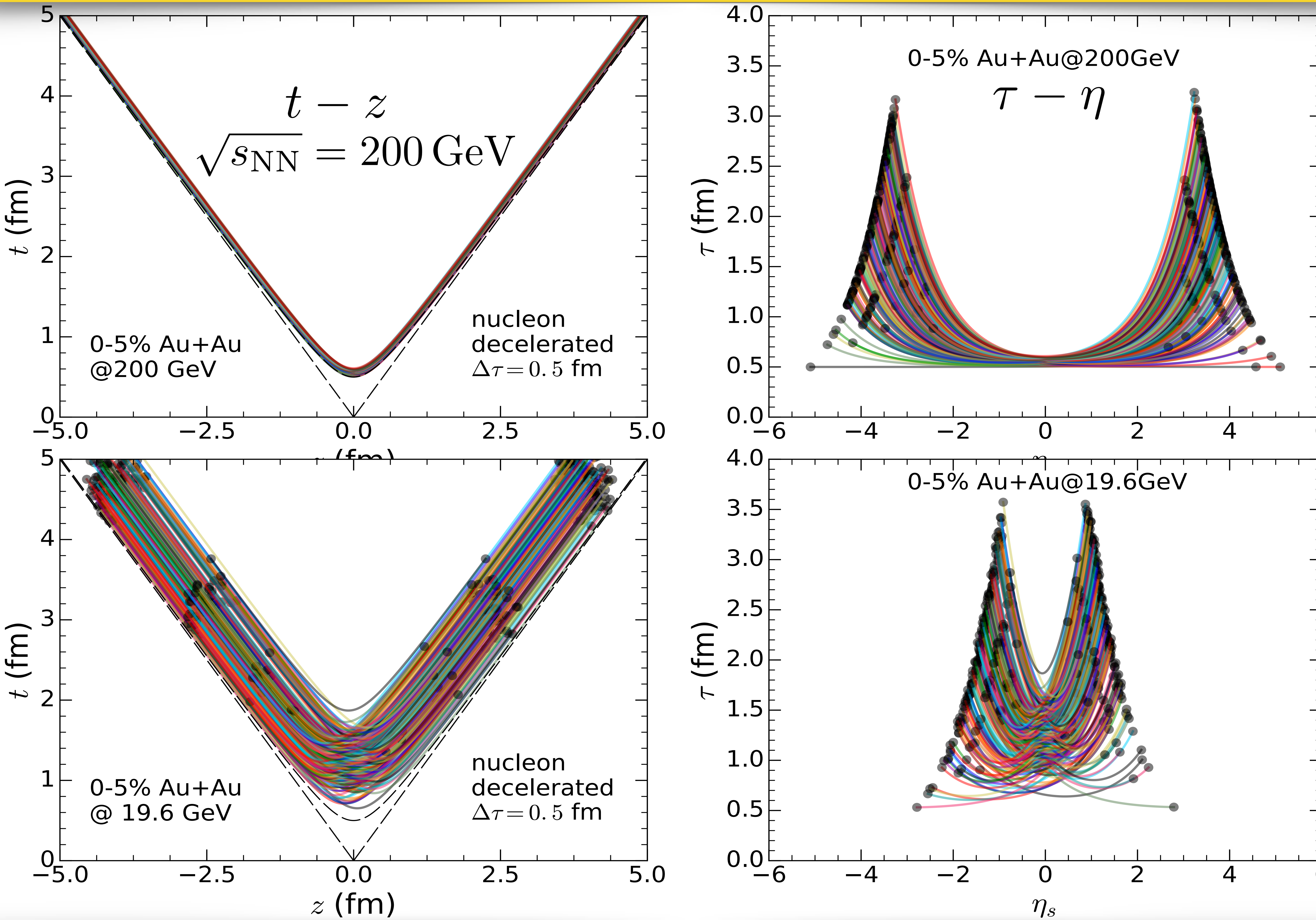

Hydrodynamics with sources

Energy-momentum current and net baryon density are feed into hydrodynamic simulation as source terms

$$\partial_\mu T^{\mu\nu} = J^\nu_{\mathrm{source}}$$

$$\partial_\mu J^\mu = \rho_{\mathrm{source}}$$

where

$$J^\nu_{\mathrm{source}} = \delta e u^\nu + (e + P)\delta u^\nu$$

$$\delta u^\nu = \frac{\Delta^\nu_\mu J^\mu_{\mathrm{source}}}{e + P}$$

heats up the system — accelerates the flow velocity

ρ_{source} dopes baryon charges into the system

- Source terms are smeared with Gaussians in space and time

Hydrodynamical evolution with sources

energy density

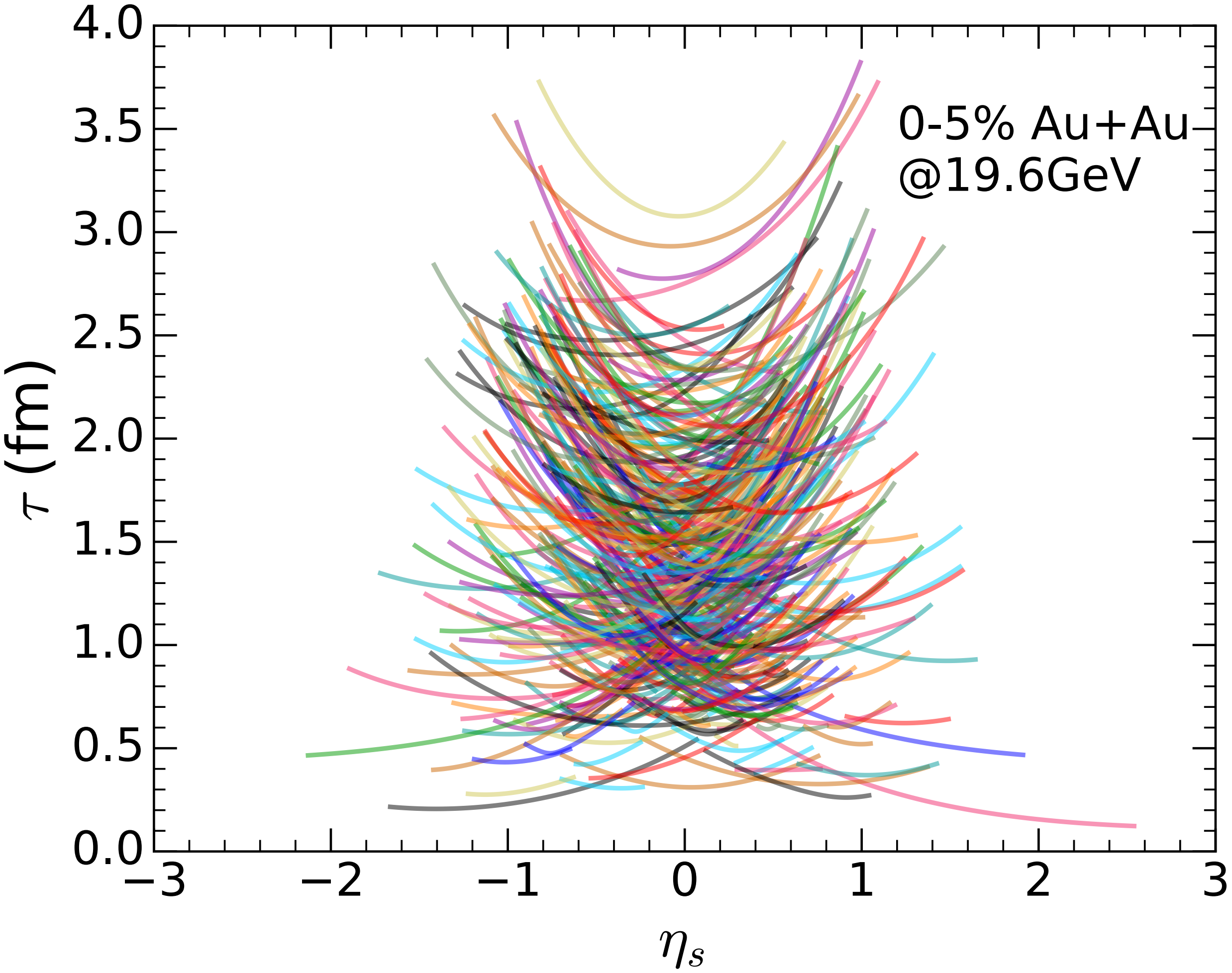

$$\sqrt{s_{\mathrm{NN}}} = 19.6\,\mathrm{GeV}$$

valence quark +
rapidity loss fluct.

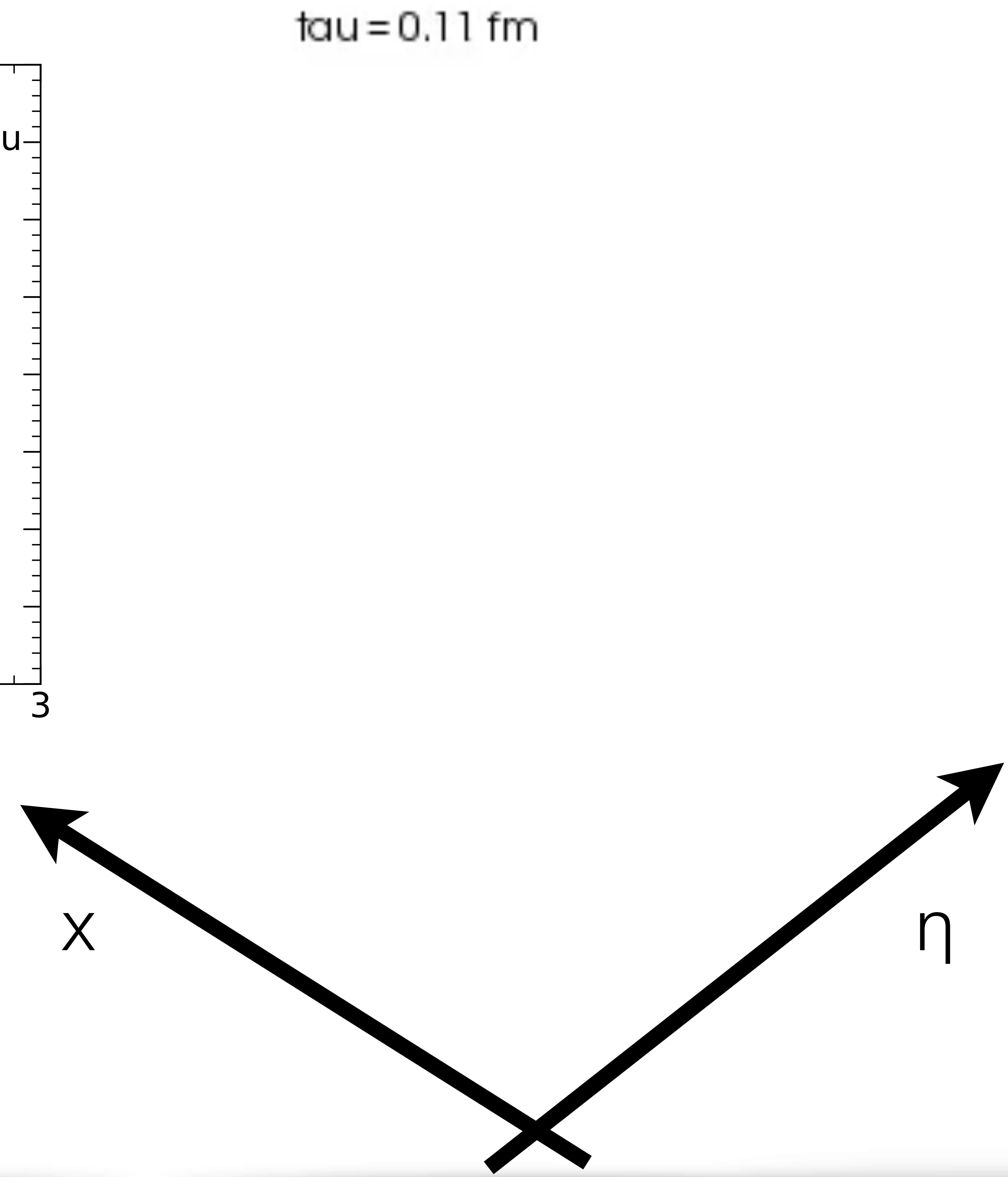

Hydrodynamical evolution with sources

net baryon density

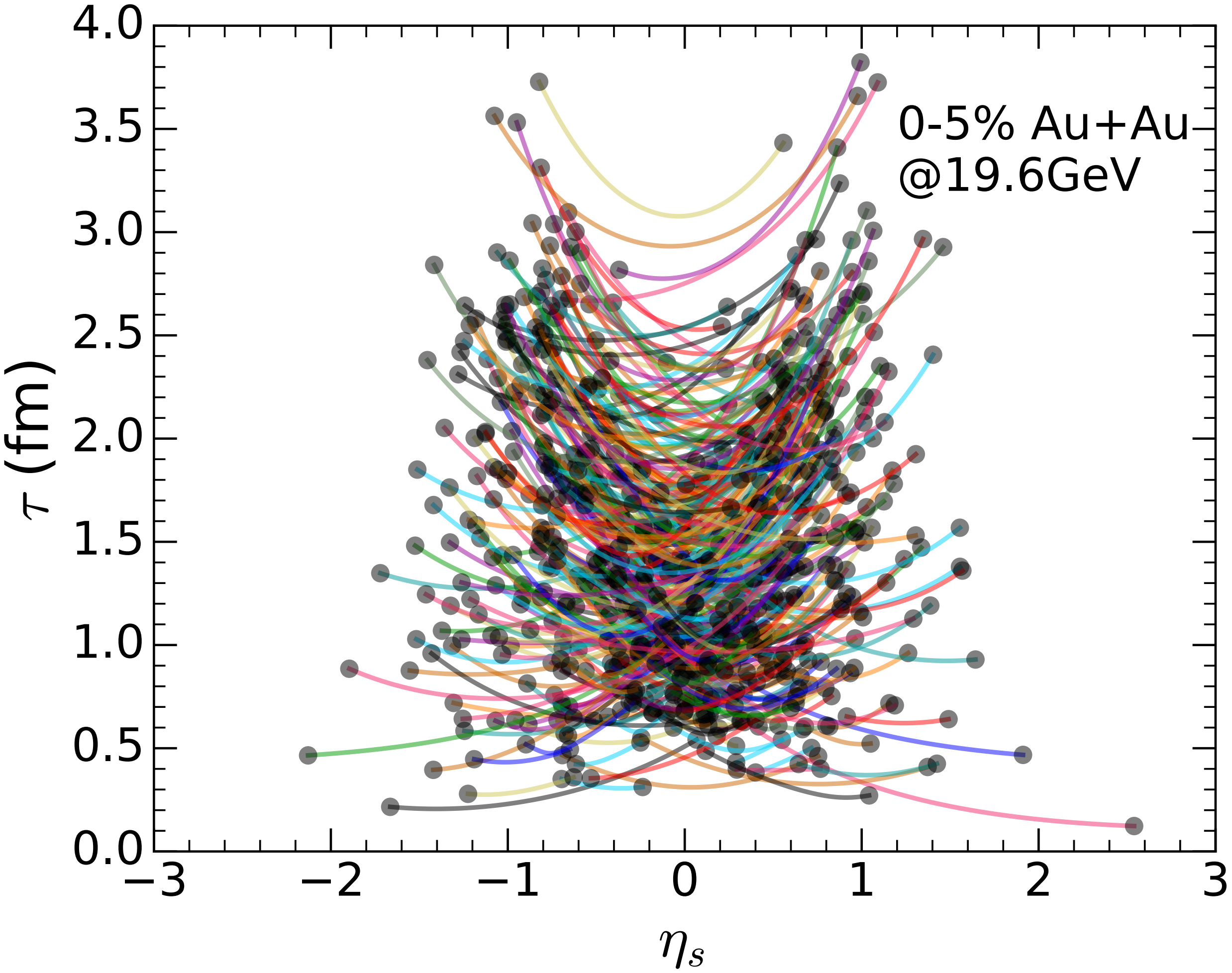

tau=0.11 fm

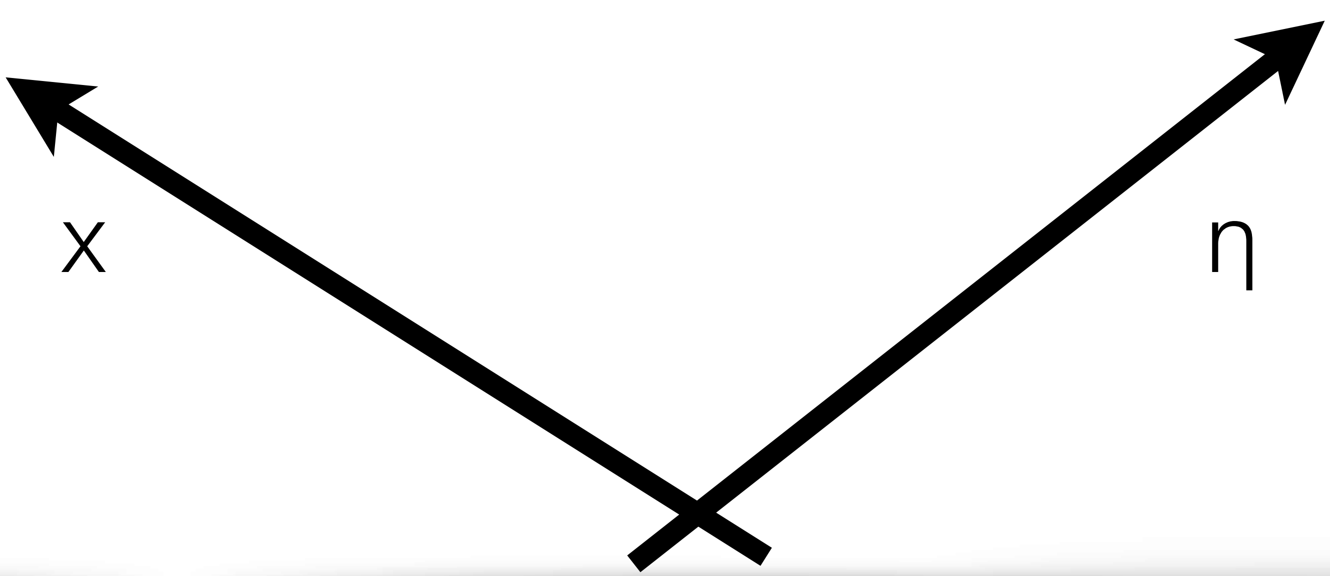

$$\sqrt{s_{\mathrm{NN}}} = 19.6\,\mathrm{GeV}$$

valence quark +
rapidity loss fluct.

Particle rapidity distribution

C. Shen and B. Schenke, arXiv:1710.00881 [nucl-th].

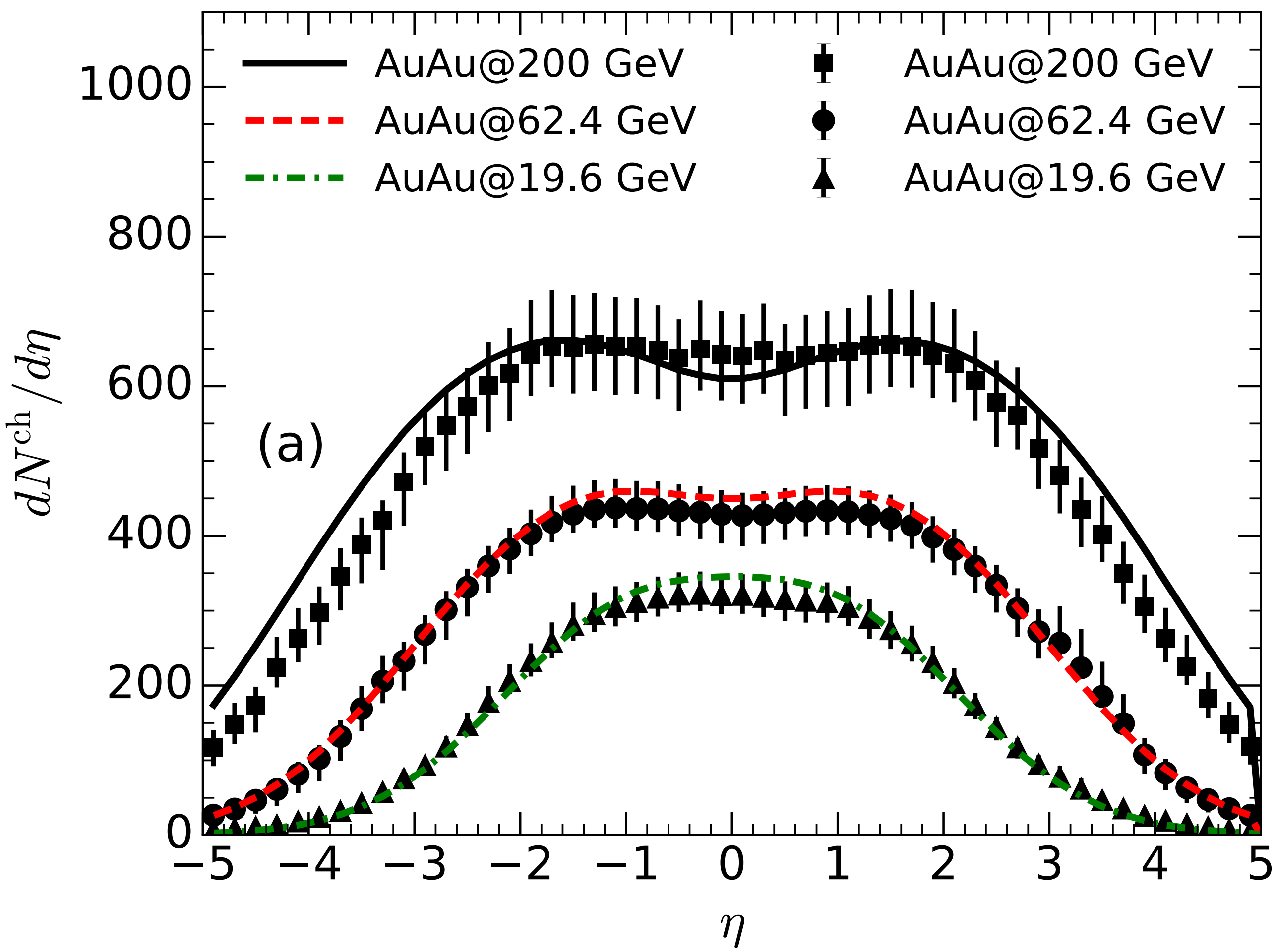

- Rapidity distribution of charged hadrons agrees fairly good with the RHIC BES measurements below 62.4 GeV

Particle rapidity distribution

C. Shen and B. Schenke, arXiv:1710.00881 [nucl-th].

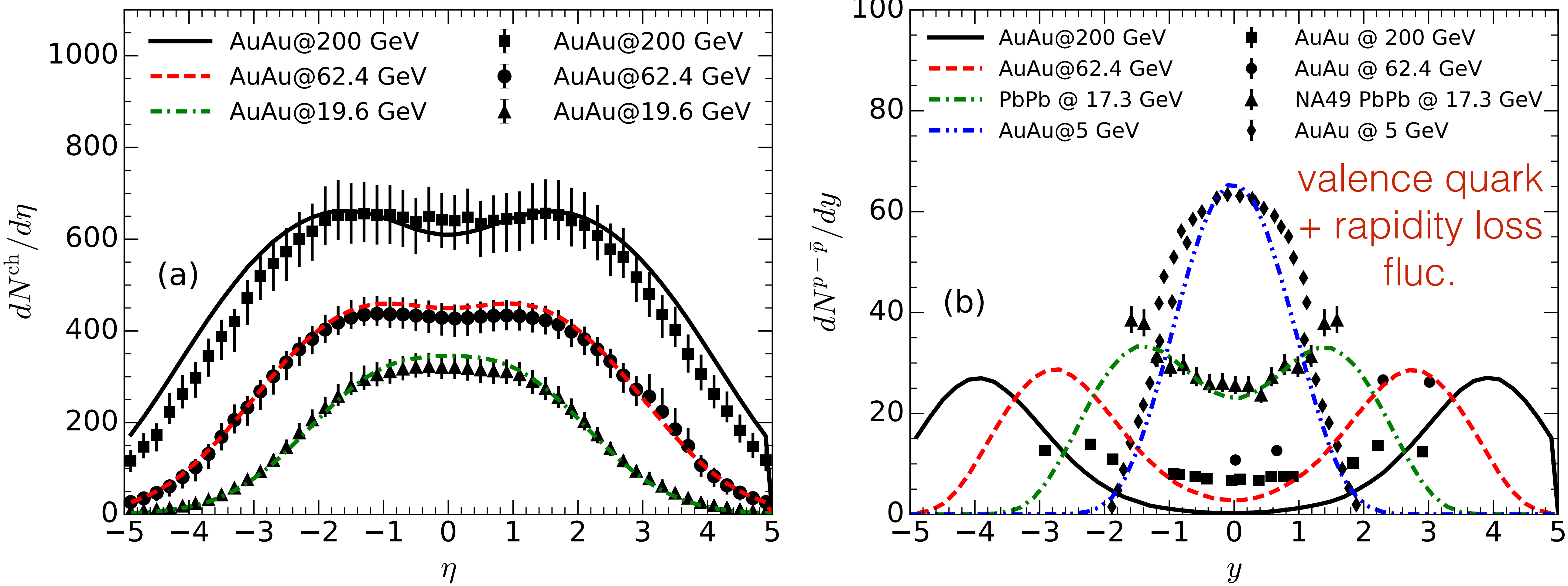

- Rapidity distribution of charged hadrons agrees fairly good with the RHIC BES measurements below 62.4 GeV
- Net proton rapidity distributions are reasonably reproduced at low BES energy; but too low for high energies

Hydrodynamics with baryon diffusion

Dissipative hydrodynamics

C. Shen, G. Denicol, C. Gale, S. Jeon, A. Monnai, B. Schenke, in preparation

Energy momentum tensor

$$T^{\mu\nu} = e u^\mu u^\nu - (P + \Pi)\Delta^{\mu\nu} + \pi^{\mu\nu}$$

$$\Delta^{\mu\nu} = g^{\mu\nu} - u^\mu u^\nu$$

Conserved currents

$$J^\mu = n u^\mu + q^\mu$$

New!

Equations of motion

$$\partial_\mu T^{\mu\nu} = 0$$
$$\partial_\mu J^\mu = 0$$
$$+ \quad P(e, n)$$

Dissipative quantities are evolved with 2nd order Israel-Stewart type of equations

At Navier-Stokes limit,

$$\pi^{\mu\nu} \sim 2\eta \nabla^{\langle\mu} u^{\nu\rangle} \quad \Pi \sim -\zeta \partial_\mu u^\mu \quad q^\mu \sim \kappa \nabla^\mu \frac{\mu}{T}$$

$$\nabla^\mu = \Delta^{\mu\nu}\partial_\nu$$

Effects of net baryon diffusion on particle yields

C. Shen, G. Denicol, C. Gale, S. Jeon, A. Monnai, B. Schenke, in preparation

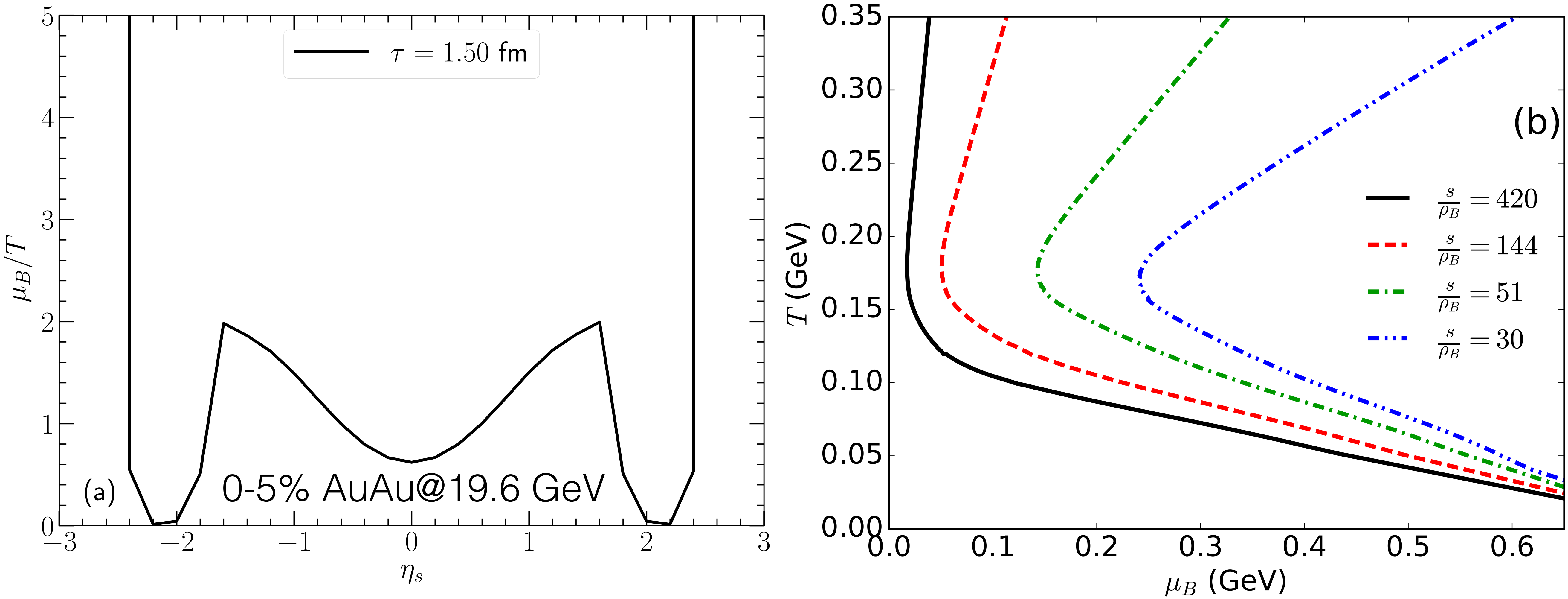

- The value of μ_B/T increases at low density regions
- The spatial gradients of μ_B/T drive the net baryon diffusion current to work against the hydrodynamic radial flow

Effects of net baryon diffusion on particle yields

C. Shen, G. Denicol, C. Gale, S. Jeon, A. Monnai, B. Schenke, in preparation

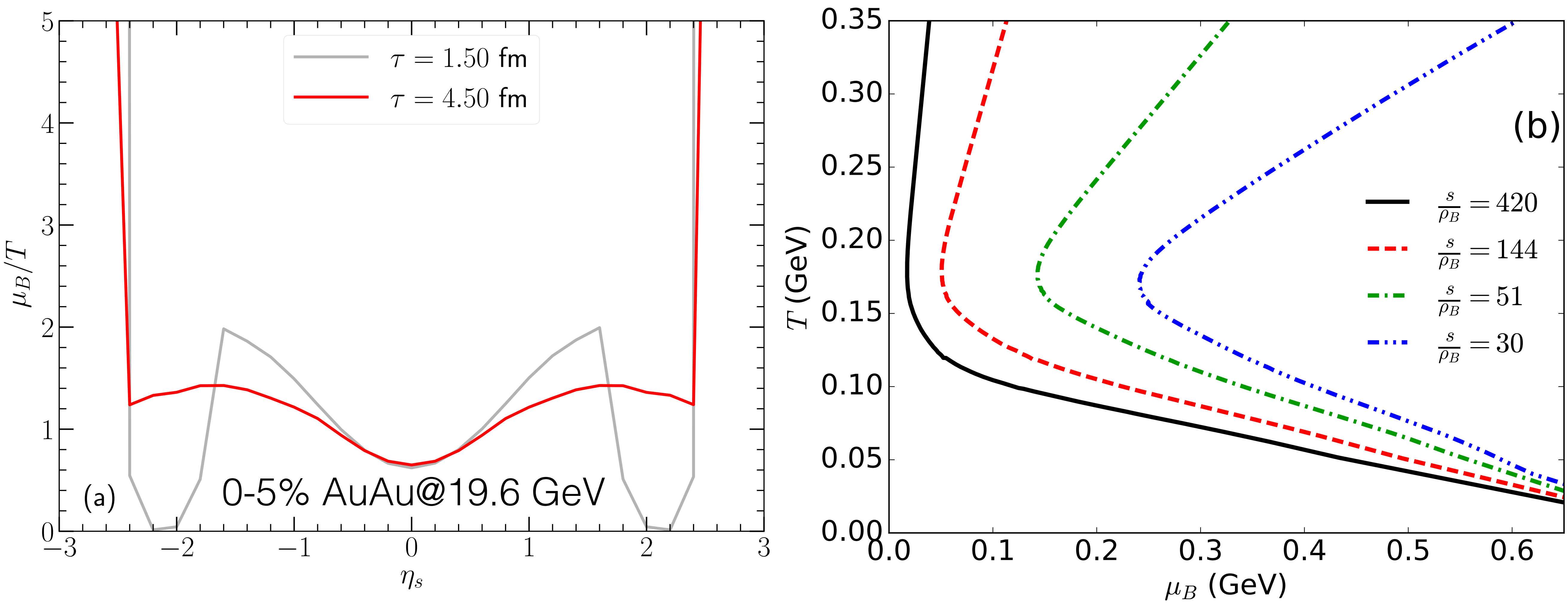

- The value of μ_B/T increases at low density regions
- The spatial gradients of μ_B/T drive the net baryon diffusion current to work against the hydrodynamic radial flow

Effects of net baryon diffusion on particle yields

C. Shen, G. Denicol, C. Gale, S. Jeon, A. Monnai, B. Schenke, in preparation

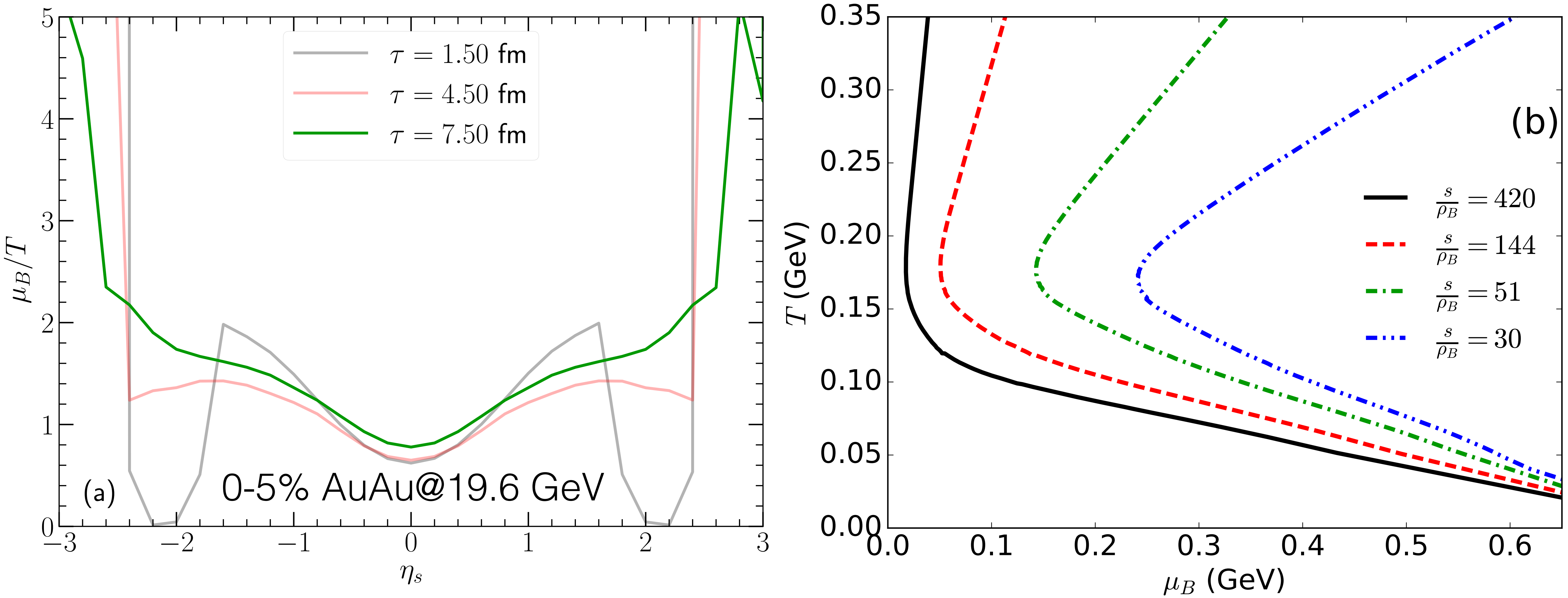

- The value of μ_B/T increases at low density regions
- The spatial gradients of μ_B/T drive the net baryon diffusion current to work against the hydrodynamic radial flow

Effects of net baryon diffusion on particle yields

C. Shen, G. Denicol, C. Gale, S. Jeon, A. Monnai, B. Schenke, in preparation

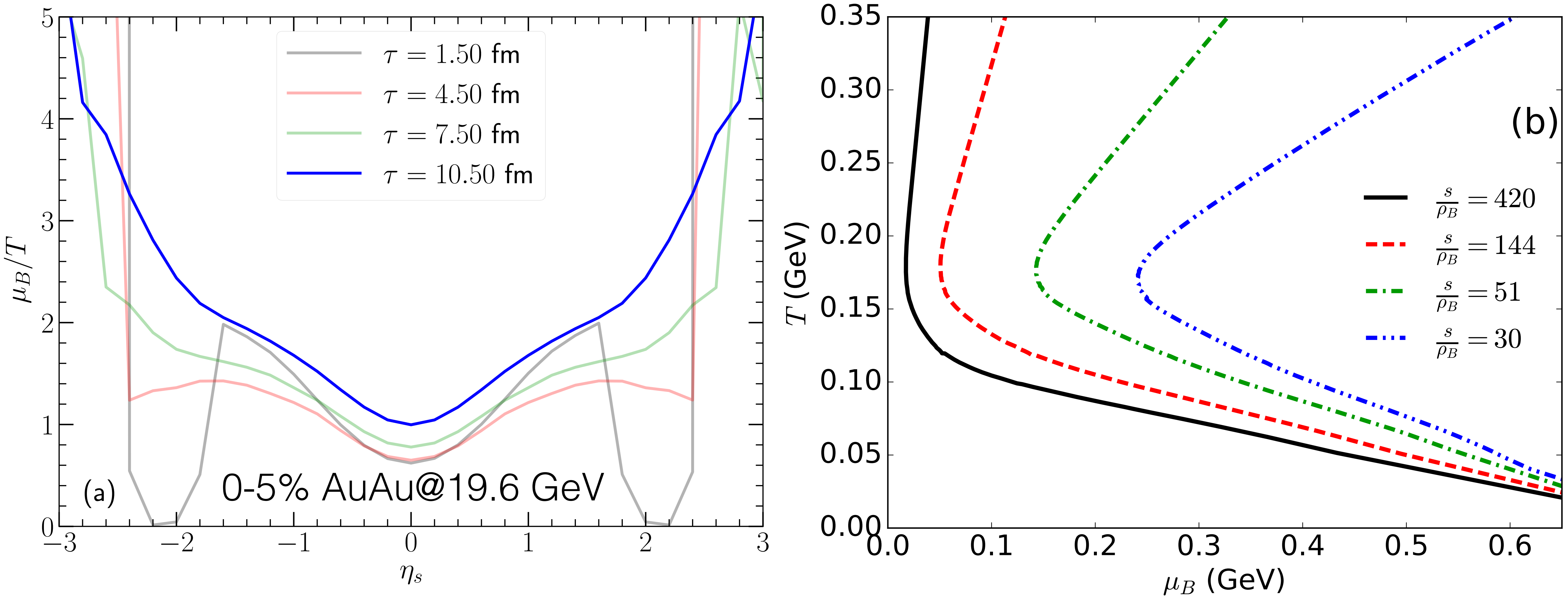

- The value of μ_B/T increases at low density regions
- The spatial gradients of μ_B/T drive the net baryon diffusion current to work against the hydrodynamic radial flow

Effects of net baryon diffusion on particle yields

C. Shen, G. Denicol, C. Gale, S. Jeon, A. Monnai, B. Schenke, in preparation

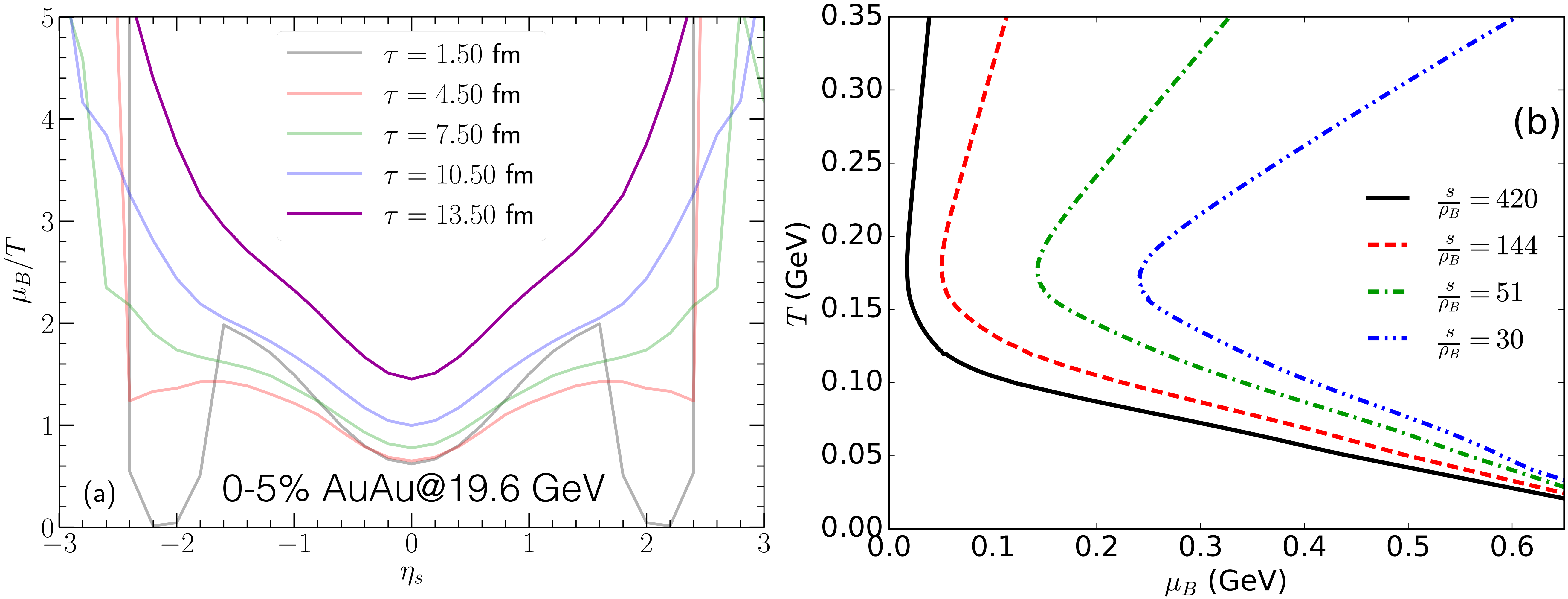

- The value of μ_B/T increases at low density regions
- The spatial gradients of μ_B/T drive the net baryon diffusion current to work against the hydrodynamic radial flow

Effects of net baryon diffusion on particle yields

C. Shen, G. Denicol, C. Gale, S. Jeon, A. Monnai, B. Schenke, in preparation

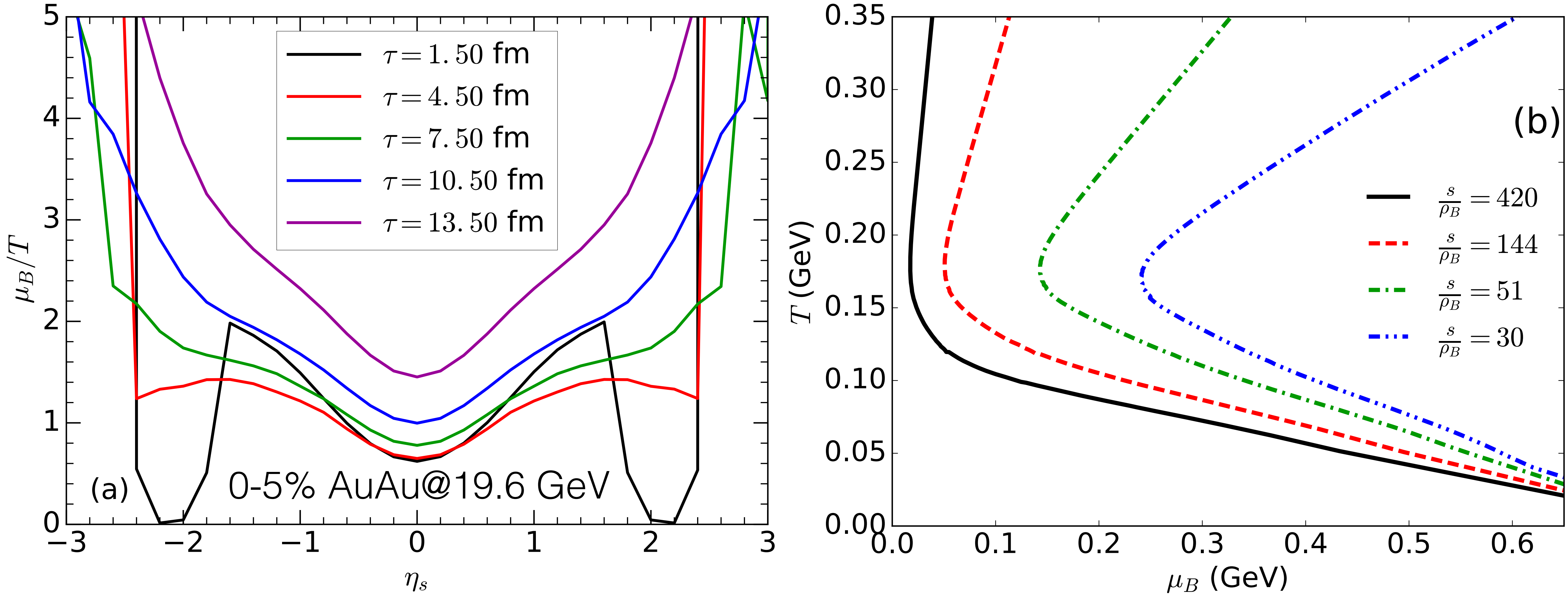

- The value of μ_B/T increases at low density regions
- The spatial gradients of μ_B/T drive the net baryon diffusion current to work against the hydrodynamic radial flow

Effects of net baryon diffusion on particle yields

C. Shen, G. Denicol, C. Gale, S. Jeon, A. Monnai, B. Schenke, in preparation

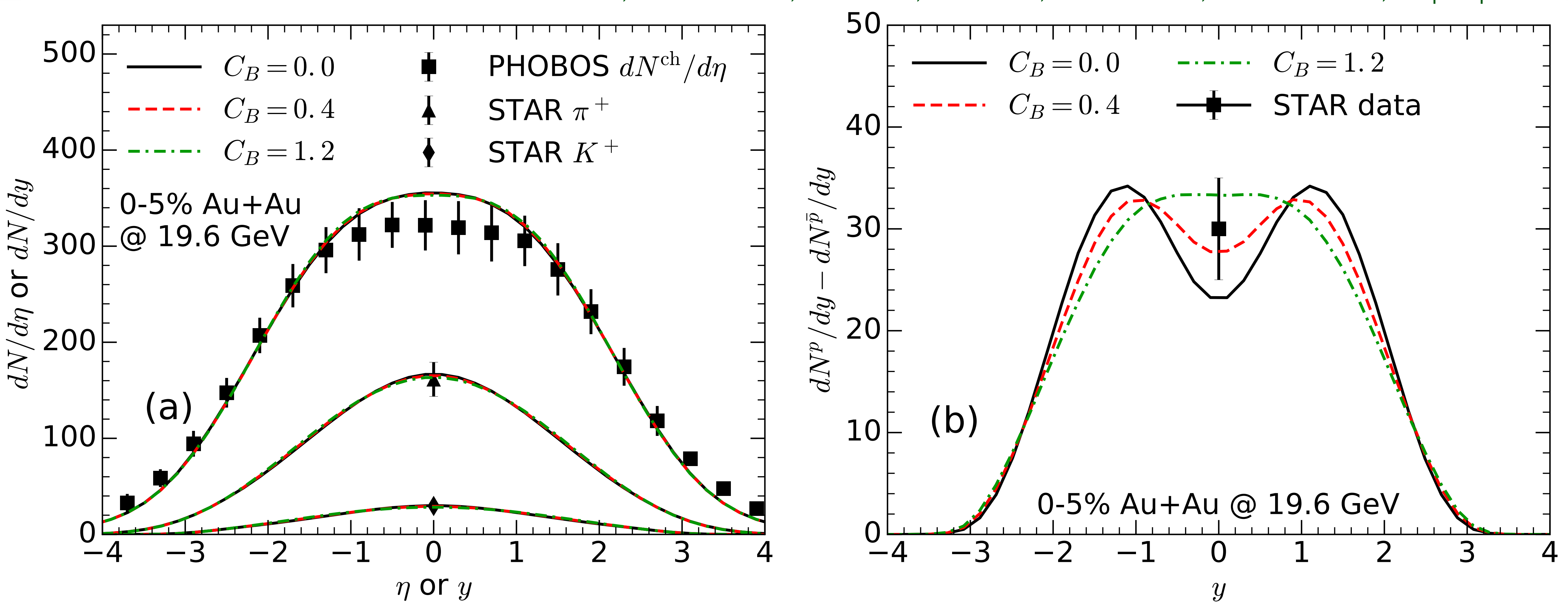

$$\kappa_B = \frac{C_B}{T}\rho_B\left(\frac{1}{3}\coth\left(\frac{\mu_B}{T}\right) - \frac{\rho_B T}{e+P}\right)$$

- More net baryon numbers are transported to mid-rapidity with a larger diffusion constant

Constraints on net baryon diffusion and initial condition

Effects of net baryon diffusion on particle yields

C. Shen, G. Denicol, C. Gale, S. Jeon, A. Monnai, B. Schenke, in preparation

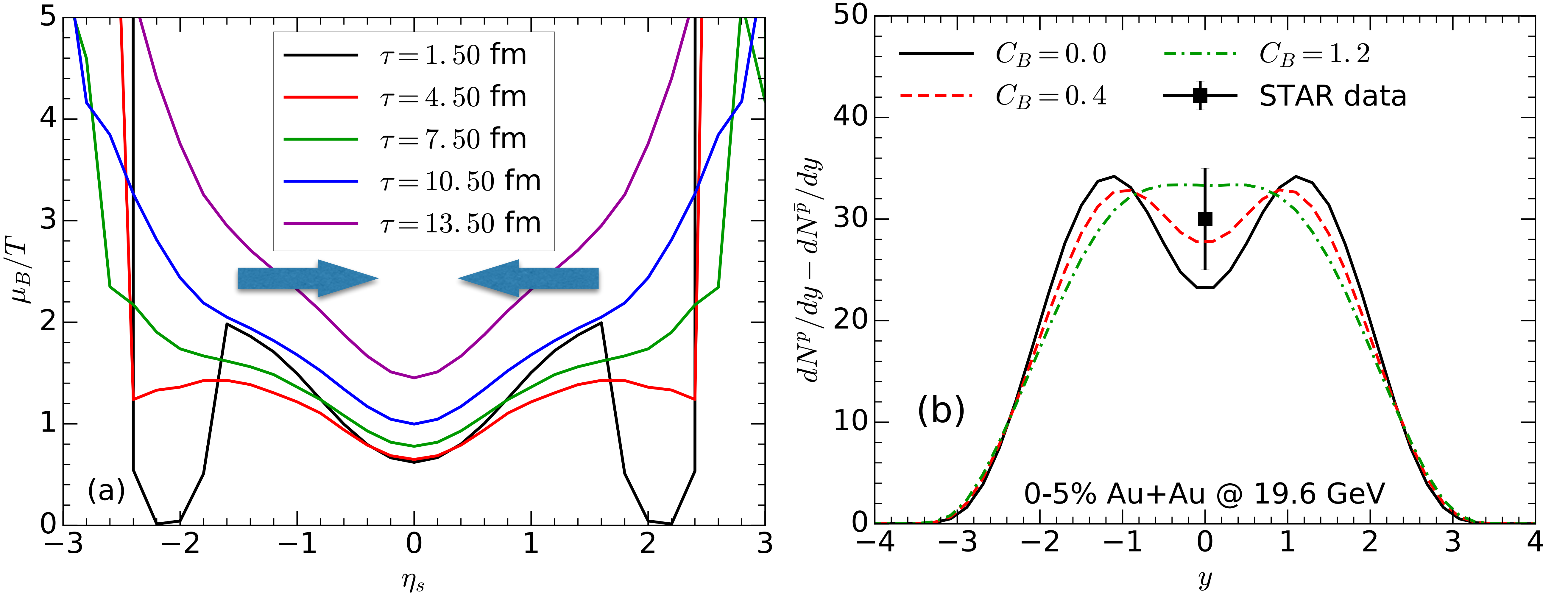

$$\kappa_B = \frac{C_B}{T}\rho_B\left(\frac{1}{3}\coth\left(\frac{\mu_B}{T}\right) - \frac{\rho_B T}{e+P}\right)$$

- More net baryon numbers are transported to mid-rapidity with a larger diffusion constant

Constraints on net baryon diffusion and initial condition

Conclusion

- Event-by-event viscous hydrodynamics is an effective macroscopic theory for high energy heavy-ion collisions

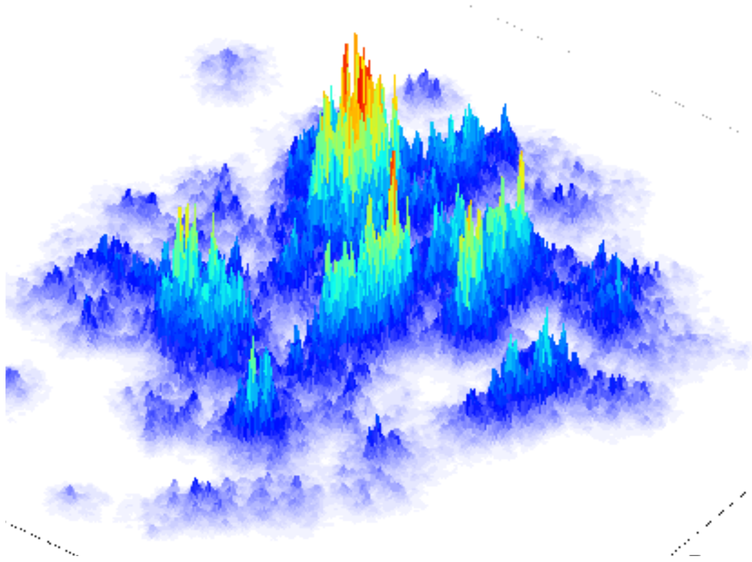

$\frac{\eta}{s}, \frac{\zeta}{s}, \kappa_B$, and more …

- We develop a dynamical initialization framework to study the early time evolution of heavy-ion collisions at the RHIC BES energies

Baryon stopping
Mapping the QCD phase diagram